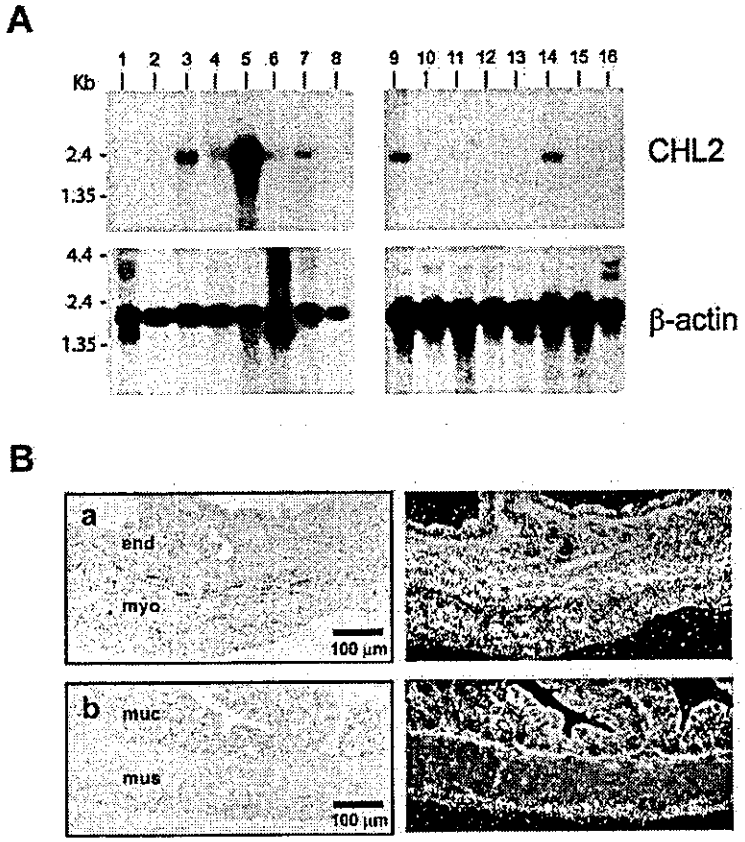

Fig. 5. Expression of CHL2 mRNA in soft tissues. (A) Northern blot analyses with human multiple tissue blots IV (lanes 1-8) and I (lanes 9-16) are shown. Blots were first probed with a DNA containing the *hCHL2* ORF (CHL2), and then re-probed with human β-actin (Clontech). Essentially identical results were achieved with three different blot batches. Lane 1, spleen; lane 2, thymus; lane 3, prostate; lane 4, testis; lane 5, uterus (without endometrium); lane 6, small intestine; lane 7, colon; lane 8, peripheral blood leukocytes; lane 9, heart; lane 10, whole brain; lane 11, placenta; lane 12, lung; lane 13, liver; lane 14, skeletal muscle; lane 15, kidney; lane 16, pancreas. (B) In situ hybridization for *CHL2* in adult mouse tissues, shown in paired bright-field (left) and dark-field (right) panels. (a) Uterus (transverse section) showing *CHL2* expression primarily in the myometrium. (b) Colon, showing weak *CHL2* expression in serosal cells – a different pattern to that of *CHL1* (Nakayama et al., 2001). muc, submucosa; mus, muscularis; end, endometrium; myo, myometrium.

was sufficient to enlarge the particle size, did not affect the degree of mineralization.

Taken together, these results suggest that CHL2 induction in damaged joint cartilage may reduce the extent or speed of hypertrophic differentiation in articular chondrocytes.

Table 5. Reduced levels of cartilage matrix mineralization in the presence of CHL2

Factors*	Mineralizing cartilage† (% total)	Weak-positive‡ (% total)	Negative§ (% total)
none	5 (71.5)	2 (28.5)	0 (0)
noggin-Fc	1 (25)	2 (50)	1 (25)
mCHL2-FLAG	2 (25)	3 (37.5)	3 (37.5)
BMP6	3 (75)	1 (25)	0 (0)

ES cell-derived mesodermal progenitor cells were cultured as a pellet for 18 days and then induced to mineralize for 6-8 days. Cartilage particles were fixed, sectioned, stained with von Kossa, and classified on the basis of the degrees of mineral deposition in matrix. Occasional strong von Kossa staining on the non-cartilaginous surface layer of the particles was not considered to be cartilage mineralization.

*2 μg/ml (40 nM) noggin-Fc, 3 μg/ml (64.5 nM) mCHL2-FLAG, 50 ng/ml (1.7 nM) BMP6 were added on day 15.

†Particles containing areas of cartilaginous extracellular matrix that stained with von Kossa (Fig. 7Ca). The von Kossa-positive areas were located adjacent to the surface cell layer, which was COL2/COL10-negative and thereby non-cartilaginous (Fig. 7Cb).

‡Particles containing smaller von Kossa-positive nodules.

§Particles containing no von Kossa-positive areas or a very small von Kossa-positive spot inside the particle (Fig. 7Cd,g).

Discussion

We have demonstrated here that CHL2, the second chordin-like gene, encodes a protein that directly interacts with different BMPs, inhibiting their actions in vitro as well as in vivo in a manner similar to chordin, noggin and CHL1. Expression analysis suggests a possible role for CHL2 during formation and maintenance of articular cartilage and reproductive organs. We have also provided evidence that CHL2 might negatively regulate cartilage formation/regeneration in diseased joints.

Structure and function of CHL2

Searches of human and mouse genome databases indicated that CHL2 is most homologous to CHL1. Injection of CHL2 RNA induced trunk duplication in early *Xenopus* embryos similar to those produced by chordin and CHL1(s2) RNAs (Table 2) (Nakayama et al., 2001). Recombinant mCHL2 protein interacted directly with five BMPs and one GDF (Fig. 2 and Nakayama et al., 2001) thereby inhibiting, in vitro, several BMP/GDF-dependent processes including, osteogenic differentiation of C2C12 mesenchymal progenitor cells by several BMPs (Fig. 3, Table 3), ATDC5 embryonal carcinoma cells by GDF5 (not shown) and BMP4-dependent lymphohematopoietic ($CD34^+CD31^{hi}$ and $CD34^+CD31^{lo}$) progenitor cell development from ES cells (not shown) (Nakayama et al., 2000). Under our conditions, CHL2 provided 50% inhibition (IC50) by blocking a half to a third of available BMP dimers, suggesting that tight CHL2 binding to one BMP subunit might be sufficient for full inhibition. Furthermore, as with related factors (chordin, noggin, CHL1), CHL2 prevented BMP interactions with the BMP receptor (Fig. 2C), although CHL2 activity was two- to sevenfold more potent than chordin (Table 3) and CHL1 (not shown). Thus, CHL2 is structurally and functionally similar to chordin and CHL1.

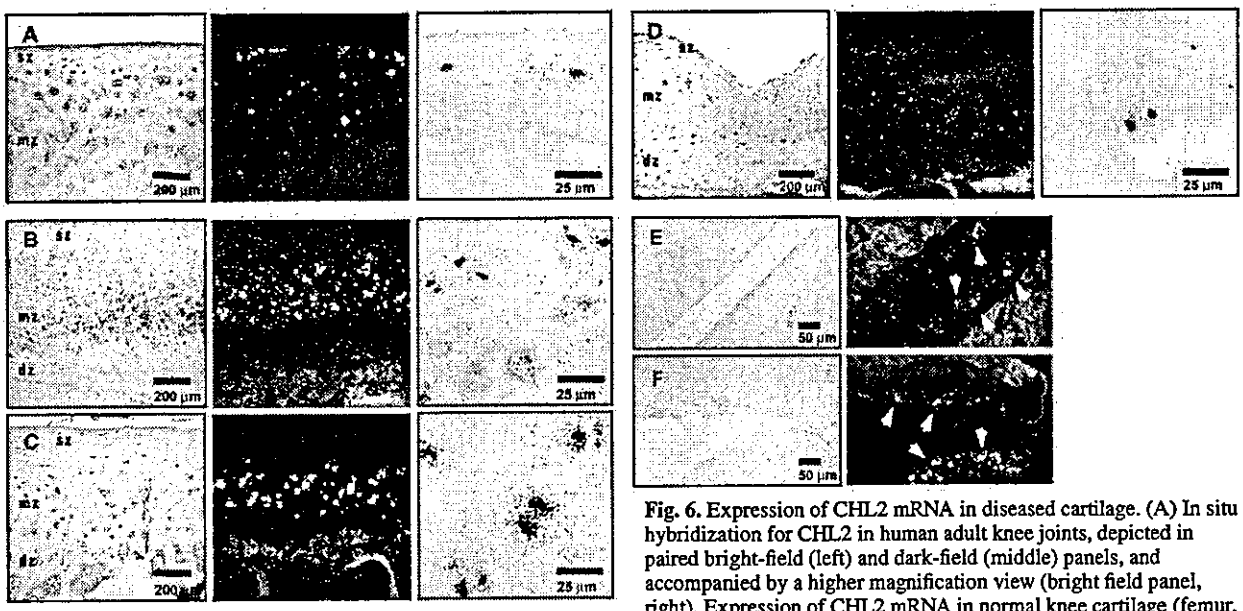

Fig. 6. Expression of CHL2 mRNA in diseased cartilage. (A) In situ hybridization for CHL2 in human adult knee joints, depicted in paired bright-field (left) and dark-field (middle) panels, and accompanied by a higher magnification view (bright field panel, right). Expression of CHL2 mRNA in normal knee cartilage (femur, 55-year old female). Note that *CHL2* is localized on articular chondrocytes (right). However, CHL2$^+$ chondrocytes are scattered throughout the cartilage. Weak signals are also visible in superficial zone chondrocytes. (B,C) Expression of *CHL2* in osteoarthritic (OA) knee cartilage (B: 73-year-old male with OA, degenerative joint disease (DJD), and chronic proliferative synovitis; C: 48-year-old female with DJD). Signal is strongly induced in middle zone chondrocytes, but absent in superficial zone chondrocytes. (D) Expression of *CHL2* in rheumatoid arthritic knee cartilage (80-year-old female with RA). Weakly positive chondrocytes are scattered throughout the cartilage. (E,F) Expression of CHL2 mRNA in hind paws of rats with collagen-induced arthritis, depicted in paired bright-field (left) and dark-field (middle) panels. CHL2 signal is weakly expressed in normal chondrocytes (E), and is not substantially elevated in animals with severe immune-mediated disease (F). Arrowheads indicate CHL2-positive chondrocytes. sz, superficial zone; mz, middle zone; dz, deep zone.

Potential roles of CHL2 in joint formation

Cartilages within hip and knee joints and at the costochondral junction were the major CHL2 expression sites during embryogenesis (Fig. 4). CHL2 mRNA was also expressed strongly in connective tissues anchoring reproductive organs (Fig. 5). CHL2 in developing joints was restricted to superficial zone chondrocytes; expression was substantially diminished in adult joint cartilage (Fig. 4). The CHL2-expressing areas did not overlap domains expressing chordin (non-chondrogenic mesenchyme of limb buds), CHL1 (condensing mesoderm, hypertrophic chondrocytes) and gremlin (non-chondrogenic regions of limb buds, including interdigital mesenchyme) during limb formation (Nakayama et al., 2001; Scott et al., 1999; Scott et al., 2000), suggesting that these four factors have divergent biological roles. However, as with CHL1 (Nakayama et al., 2001), CHL2 expression in developing cartilage overlapped with noggin expression (Brunet et al., 1998; Capdevila and Johnson, 1998; Merino et al., 1998; Nifuji and Noda, 1999; Pathi et al., 1999).

As CHL2 is a BMP-binding inhibitor, and BMPs regulate multiple steps during chondrogenesis, expression of CHL2 in superficial chondrocytes in developing joints suggests a role in joint specification. The ability of exogenous mCHL2 to inhibit chondrogenesis by hMSCs supports this hypothesis (Fig. 7A,B, Table 4). The surface of developing cartilage consists of proliferating mesenchymal cell layers that are differentiating into chondrocytes. By its location, CHL2 might act as an important boundary in joint formation. A possible role could be to prevent articular cartilage from becoming too massive, by keeping mesenchymal cells in the joint space from being recruited to the chondrocyte developmental pathway.

Alternatively, CHL2 could play more subtle roles. The superficial zone of articular cartilage is composed of flattened chondrocytes separated by tangential arrays of thin collagen fibrils, but no proteoglycan matrix. In contrast, the middle zone consists of rounded chondrocytes surrounded by a proteoglycan-rich matrix containing radial bundles of thick collagen fibrils. Osteogenic BMPs accumulate in the pericellular matrix of articular cartilage, with highest levels in the middle to deep zone (Anderson et al., 2000). Conversely, the osteogenic antagonist BMP3 (Daluiski et al., 2001) is more highly expressed in the superficial zone. We failed to detect an interaction between CHL2 and BMP3 (not shown), suggesting that preferential expressions of CHL2 and BMP3 in the surface chondrocytes act to regulate a BMP gradient in normal articular cartilage.

Potential involvement of CHL2 in osteoarthritis

CHL2 mRNA was never detected in the growth plate, where proliferation and hypertrophic differentiation of pre-hypertrophic chondrocytes normally occur, implying that CHL2 is not relevant to normal pathways of chondrocyte proliferation and maturation. However, the up-regulation of CHL2 transcripts specifically in middle zone cartilage of adult joints with OA (Fig. 6) prompted our speculation that CHL2 has a role in cartilage repair. We examined the associations between CHL2 and three principal phenotypes of OA cartilage: (1) reduced proteoglycan levels (which precede overt

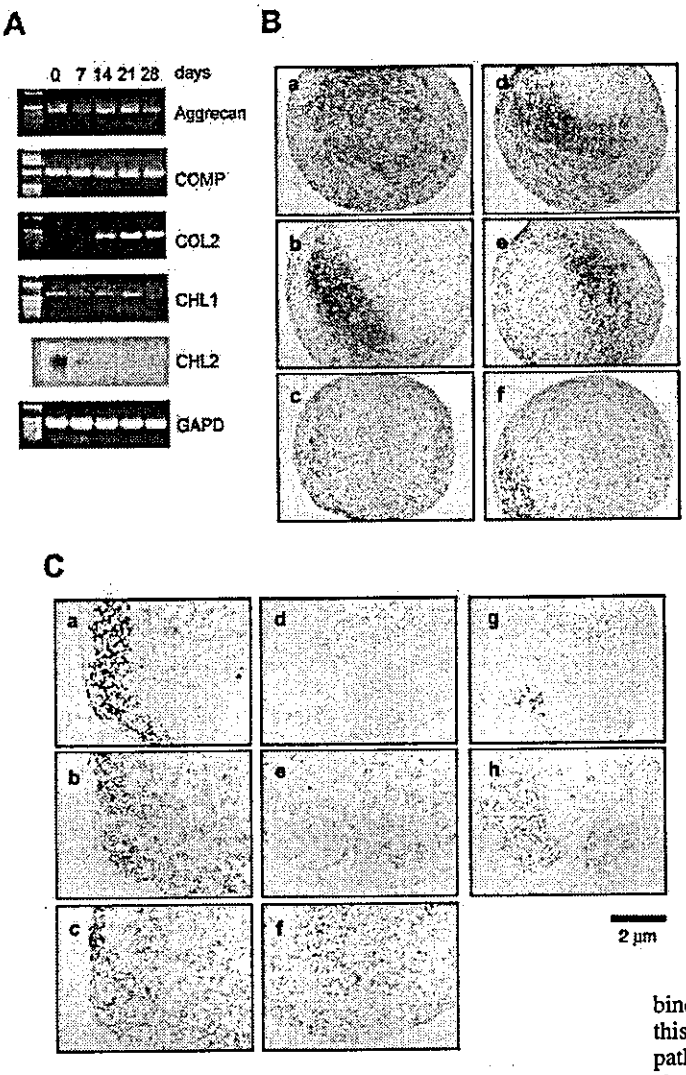

Fig. 7. Effect of CHL2 on in vitro chondrogenesis. (A) CHL mRNA expression during chondrogenic culture. hMSCs were grown in pellet culture in the presence of TGFβ3. On the indicated day, RNA was extracted from particles, treated with DNase I, and subjected to RT-PCR using primers for aggrecan, COMP, COL2, CHL1, CHL2 and GAPD. The CHL2 signal was confirmed with a ^{33}P-labeled *XbaI-SalI* fragment from pSPORThCHL2. (B) hMSCs were grown in pellet culture in the presence of TGFβ3 alone (a,d), or TGFβ3 with either 0.2 µg/ml mCHL2-FLAG (b), 2 µg/ml mCHL2-FLAG (c), 0.1 µg/ml noggin-Fc (e), or 1 µg/ml noggin-Fc (f). On day 21, particles were harvested and stained with Toluidine Blue. Data are representative of five independent experiments. Addition of IgG-Fc did not affect growth and maturation of cartilage-containing particles (not shown). Note that cartilage nodules, in which well-separated cells were embedded, stained more intensely with Toluidine Blue. (C) Effect of CHL2 on in vitro mineralization of EB cell-derived cartilage. FACS-purified FLK1$^-$PDGFRα$^+$ EB cells were grown in pellet micromass culture to produce hyaline cartilage particles. On day 18, the medium was changed to a hypertrophic differentiation medium in the absence (a-c) or presence of 3 µg/ml mCHL2-FLAG (d-f) or 2 µg/ml noggin-Fc (g,h). On day 24, particles were harvested, stained with von Kossa (a,d,g), and immunostained with X53 for COL10 (b,e,h) or 2B1.5 for COL2 (c,f). Data are representative of four independent experiments. The Scale bar for B and C is shown in C.

histological changes), (2) aberrant chondrocyte proliferation (resulting in clonal chondrocyte expansion), and (3) upregulation of molecules (e.g., COL1, COL3, COL10, and AP) found in hypertrophied or de-differentiated chondrocytes but not normal articular chondrocytes (Aigner et al., 1993; Kirsch et al., 2000b; Von der Mark et al., 1992). First, the proteoglycan content in CHL2-expressing regions of OA cartilage was not reduced, as detected in Toluidine Blue-stained sections by the retained metachromasia (not shown). Second, CHL2-expressing chondrocytes in OA cartilage were typically found as aggregates; however, middle to deep zone chondrocytes are normally arranged in a cylindrical fashion, so this association might reflect normal middle zone anatomy. In contrast, the weak but significant inhibition of cartilage mineralization by CHL2 (Fig. 7C, Table 5) suggested that in OA cartilages this molecule might delay and/or reduce the degree of chondrocyte hypertrophy, thereby ameliorating cartilage degeneration. Further support for this premise is that medium turbidity, which indicates mineral deposition and excess Ca^{2+} excretion, was delayed during hypertrophic differentiation culture of cartilage particles by CHL2 or noggin (not shown). However, we have not addressed whether CHL2 is involved in the de-differentiation of mature articular chondrocytes. Co-localization analyses between cells expressing the CHL2 mRNA and those expressing transcripts for COL1, COL10 or proliferating cell-nuclear antigen are underway to answer this question.

In conclusion, abundant evidence suggests that BMP functions are regulated by numerous extracellular BMP-binding proteins in developing joints. Our current data support this paradigm and add a new BMP inhibitor, CHL2, to this pathway. Our findings also provide the first evidence that a chordin-like BMP-binding inhibitor might be intimately involved in the pathogenesis of degenerative joint disease.

First, we wish to acknowledge the many scientists and technicians in the Amgen Genomics and Bioinformatics groups who constructed and analyzed the nucleotide sequence databases. We greatly appreciate the superb technical support provided by R. Haldankar, H. Yamane, and M. Haniu for mid-scale mCHL2 preparation and NH_2-terminal amino acid sequence determination, and by R. Manoukian for cell sorting. We are grateful to D. Chang, L. Daugherty, C. Baikalov and H. Yamane for preparing and purifying anti-mCHL2 peptide antibodies. Finally, we warmly thank W. Boyle and S. Simonet for support and encouragement. R.N. and T.Y. are supported by Amgen Japan, K.K. Cooperative Human Tissue Network is funded by the National Cancer Institute.

References

Abreu, J. G., Ketpura, N. I., Reversade, B. and De Robertis, E. M. (2002). Connective-tissue growth factor (CTGF) modulates cell signalling by BMP and TGF-beta. *Nat. Cell Biol.* 4, 599-604.

Aigner, T., Bertling, W., Stoss, H., Weseloh, G. and Von der Mark, K.

(1993). Independent expression of fibril-forming collagens I, II, and III in chondrocytes of human osteoarthritic cartilage. *J. Clin. Invest.* **91**, 829-837.

Anderson, H. C., Hodges, P. T., Aguilera, X. M., Missana, L. and Moylan, P. E. (2000). Bone morphogenetic protein (BMP) localization in developing human and rat growth plate, metaphysis, epiphysis, and articular cartilage. *J. Histochem. Cytochem.* **48**, 1493-1502.

Balemans, W. and Van Hul, W. (2002). Extracellular regulation of BMP signaling in vertebrates: a cocktail of modulators. *Dev. Biol.* **250**, 231-250.

Brunet, L. J., McMahon, J. A., McMahon, A. P. and Harland, R. M. (1998). Noggin, cartilage morphogenesis, and joint formation in the mammalian skeleton. *Science* **280**, 1455-1457.

Capdevila, J. and Johnson, R. L. (1998). Endogenous and ectopic expression of noggin suggests a conserved mechanism for regulation of BMP function during limb and somite patterning. *Dev. Biol.* **197**, 205-217.

Coffinier, C., Tran, U., Larrain, J. and De Robertis, E. M. (2001). Neuralin-1 is a novel Chordin-related molecule expressed in the mouse neural plate. *Mech. Dev.* **100**, 119-122.

Daluiski, A., Engstrand, T., Bahamonde, M. E., Gamer, L. W., Agius, E., Stevenson, S. L., Cox, K., Rosen, V. and Lyons, K. M. (2001). Bone morphogenetic protein-3 is a negative regulator of bone density. *Nat. Genet.* **27**, 84-88.

Garcia Abreu, J., Coffinier, C., Larrain, J., Oelgeschlager, M. and De Robertis, E. M. (2002). Chordin-like CR domains and the regulation of evolutionarily conserved extracellular signaling systems. *Gene.* **287**, 39-47.

Grimsrud, C. D., Romano, P. R., D'Souza, M., Puzas, J. E., Reynolds, P. R., Rosier, R. N. and O'Keefe, R. J. (1999). BMP-6 is an autocrine stimulator of chondrocyte differentiation. *J. Bone Miner. Res.* **14**, 475-482.

Harlow, E. and Lane, D. (1988). *Antibodies: A Laboratory Manual.* Cold Spring Harbor, NY: Cold Spring Harbor Laboratory Press.

Jaiswal, N., Haynesworth, S. E., Caplan, A. I. and Bruder, S. P. (1997). Osteogenic differentiation of purified, culture-expanded human mesenchymal stem cells in vitro. *J. Cell. Biochem.* **64**, 295-312.

Kirsch, T., Nickel, J. and Sebald, W. (2000a). BMP-2 antagonists emerge from alterations in the low-affinity binding epitope for receptor BMPR-II. *EMBO J.* **19**, 3314-3324.

Kirsch, T., Swoboda, B. and Nah, H. (2000b). Activation of annexin II and V expression, terminal differentiation, mineralization and apoptosis in human osteoarthritic cartilage. *Osteoarthritis Cartilage* **8**, 294-302.

Larrain, J., Bachiller, D., Lu, B., Agius, E., Piccolo, S. and De Robertis, E. M. (2000). BMP-binding modules in chordin: a model for signalling regulation in the extracellular space. *Development* **127**, 821-830.

Mackay, A. M., Beck, S. C., Murphy, J. M., Barry, F. P., Chichester, C. O. and Pittenger, M. F. (1998). Chondrogenic differentiation of cultured human mesenchymal stem cells from marrow. *Tissue Eng.* **4**, 415-428.

Merino, R., Ganan, Y., Macias, D., Economides, A. N., Sampath, K. T. and Hurle, J. M. (1998). Morphogenesis of digits in the avian limb is controlled by FGFs, TGFbetas, and noggin through BMP signaling. *Dev. Biol.* **200**, 35-45.

Nakayama, N., Fang, I. and Elliott, G. (1998). Natural killer and B-lymphoid potential in CD34+ cells derived from embryonic stem cells differentiated in the presence of vascular endothelial growth factor. *Blood* **91**, 2283-2295.

Nakayama, N., Lee, J. and Chiu, L. (2000). Vascular endothelial growth factor synergistically enhances bone morphogenetic protein-4-dependent lymphohematopoietic cell generation from embryonic stem cells in vitro. *Blood* **95**, 2275-2283.

Nakayama, N., Han, C. E., Scully, S., Nishinakamura, R., He, C., Zeni, L., Yamane, H., Chang, D., Yu, D., Yokota, T. et al. (2001). A novel chordin-like protein inhibitor for bone morphogenetic proteins expressed preferentially in mesenchymal cell lineages. *Dev. Biol.* **232**, 372-387.

Nakayama, N., Duryea, D., Manoukian, R., Chow, G. and Han, C.-y. E. (2003). Macroscopic cartilage formation with embryonic stem cell-derived mesodermal progenitor cells. *J. Cell Sci.* **116**, 2015-2028.

Nifuji, A. and Noda, M. (1999). Coordinated expression of noggin and bone morphogenetic proteins (BMPs) during early skeletogenesis and induction of noggin expression by BMP-7. *J. Bone Miner. Res.* **14**, 2057-2066.

Oostendorp, R. A. J., Medvinsky, A. J., Kusadasi, N., Nakayama, N., Harvey, K., Orelio, C., Ottersbach, K., Ploemacher, R. E., Saris, C. and Dzierzak, E. (2002). Embryonal subregion-derived stromal cell lines from novel temperature-sensitive SV40 T antigen transgenic mice support hematopoiesis. *J. Cell Sci.* **115**, 2099-2108.

Pathi, S., Rutenberg, J. B., Johnson, R. L. and Vortkamp, A. (1999). Interaction of Ihh and BMP/Noggin signaling during cartilage differentiation. *Dev. Biol.* **209**, 239-253.

Piccolo, S., Sasai, Y., Lu, B. and De Robertis, E. M. (1996). Dorsoventral patterning in Xenopus: inhibition of ventral signals by direct binding of chordin to BMP-4. *Cell* **86**, 589-598.

Piccolo, S., Agius, E., Lu, B., Goodman, S., Dale, L. and De Robertis, E. M. (1997). Cleavage of Chordin by Xolloid metalloprotease suggests a role for proteolytic processing in the regulation of Spemann organizer activity. *Cell* **91**, 407-416.

Roh, J., Xu, L., Hering, T., Yoo, J. and Johnstone, B. (2001). Modulation of bone morphogenetic protein-2 expression during in vitro chondrogenesis. *Orthopaedic Research Society 47th Annual Meeting Abstract*, 149.

Rupp, R. A., Snider, L. and Weintraub, H. (1994). Xenopus embryos regulate the nuclear localization of XMyoD. *Genes Dev.* **8**, 1311-1323.

Sakuta, H., Suzuki, R., Takahashi, H., Kato, A., Shintani, T., Iemura, S.-i., Yamamoto, T. S., Ueno, N. and Noda, M. (2001). Ventroptin: A BMP-4 antagonist expressed in a double-gradient pattern in the retina. *Science* **293**, 111-115.

Sambrook, J., Fritsch, E. F. and Maniatis, T. (1989). *Molecular Cloning: A Laboratory Manual.* Cold Spring Harbor, NY: Cold Spring Harbor Laboratory Press.

Scott, I. C., Blitz, I. L., Pappano, W. N., Imamura, Y., Clark, T. G., Steiglitz, B. M., Thomas, C. L., Maas, S. A., Takahara, K., Cho, K. W. et al. (1999). Mammalian BMP-1/Tolloid-related metalloproteinases, including novel family member mammalian Tolloid-like 2, have differential enzymatic activities and distributions of expression relevant to patterning and skeletogenesis. *Dev. Biol.* **213**, 283-300.

Scott, I. C., Steiglitz, B. M., Clark, T. G., Pappano, W. N. and Greenspan, D. S. (2000). Spatiotemporal expression patterns of mammalian chordin during postgastrulation embryogenesis and in postnatal brain. *Dev. Dyn.* **217**, 449-456.

Sheehan, D. C. and Hrapchak, B. B. (1987). *Theory and Practice of Histotechnology.* Columbus: Battelle Press.

Trentham, D. E., Townes, A. S. and Kang, A. H. (1977). Autoimmunity to type II collagen an experimental model of arthritis. *J. Exp. Med.* **146**, 857-868.

Von der Mark, K., Kirsch, T., Nerlich, A., Kuss, A., Weseloh, G., Gluckert, K. and Stoss, H. (1992). Type X collagen synthesis in human osteoarthritic cartilage: Indication of chondrocyte hypertrophy. *Arthritis Rheum.* **35**, 806-811.

Wilcox, J. N. (1993). Fundamental principles of in situ hybridization. *J. Histochem. Cytochem.* **41**, 1725-1733.

Zimmerman, L. B., De Jesus-Escobar, J. M. and Harland, R. M. (1996). The Spemann organizer signal noggin binds and inactivates bone morphogenetic protein 4. *Cell* **86**, 599-606.

Altered expression of NDST-1 messenger RNA in puromycin aminonucleoside nephrosis

KENJI NAKAYAMA, YUMIKO NATORI, TOSHINOBU SATO, TOMOYOSHI KIMURA, AKIRA SUGIURA, HIROSHI SATO, TAKAO SAITO, SADAYOSHI ITO, and YASUHIRO NATORI

TOKYO, SENDAI, and FUKUOKA, JAPAN

Sulfated portions of glycosaminoglycan (GAG) side chains in heparan sulfate proteoglycan (HSPG) are thought to play an important role in charge-dependent selectivity of glomerular filtration against plasma proteins. Heparan sulfate *N*-acethylglucosamine *N*-deacethylase/adenosine 3'-phosphate 5'-phosphosulfate: unsubstituted glucosamine *N*-sulfotransferase (NDST) is the key enzyme regulating sulfation of GAG chains. In this study we investigated transcriptional expression of NDST-1, 1 of 4 isozymes of NDST, in glomeruli of rats with puromycin aminonucleoside (PAN) nephrosis. Nephrosis was induced in rats with a single intraperitoneal injection of 150 mg/kg PAN. On days 10 and 35, expression of NDST-1 messenger RNA (mRNA) in glomeruli was analyzed with the use of Northern-blot analysis. Immunohistochemical studies were also performed with the use of monoclonal antibodies that react specifically with the *N*-sulfated portion of the GAG chain of HSPG and agrin, a major core protein of HSPG in glomerular basement membrane (GBM). In addition, we studied the expression of NDST-1 mRNA in cultured glomerular epithelial cells (GECs) and glomerular mesangial cells in the presence of PAN. On day 10, when significant proteinuria developed, the ratios of glomerular expression of NDST-1 mRNA against glyceraldehyde-phosphate dehydrogenase mRNA in PAN-treated rats were decreased to 48% ± 6% of those in controls ($P < .05$). Immunohistochemical studies revealed that staining for *N*-sulfated GAG chains of HSPG on GBM was markedly reduced on day 10 in PAN-treated rats but that staining for agrin was unchanged. In contrast, on day 35, when PAN-treated rats recovered from proteinuria, we noted no differences in glomerular expression of NDST-1 mRNA and staining intensity for *N*-sulfated GAG chains on GBM between PAN-treated rats and controls. Incubation of GECs for 24 hours in the presence of 50 ng/mL PAN resulted in the reduction of the expression of NDST-1 mRNA (67% ± 12% of those in controls, $P < .05$). In summary, we found alteration of the expression of NDST-1 mRNA, accompanying a loss of *N*-sulfated GAG chains of HSPG on GBM without changes in the core protein agrin, in the course of PAN nephrosis. These data suggest an important role for this enzyme in heparan sulfate assembly in GBM and GEC and in the pathogenesis of proteinuria in PAN nephrosis. (J Lab Clin Med 2004; 143:106-14)

From the Research Institute, International Medical Center of Japan Tokyo,Japan; the Division of Nephrology, Endocrinology and Vascular Medicine, Department of Medicine and Department of Blood Purification, Tohoku University Hospital, Sendai, Japan; and the Fourth Department of Internal Medicine, Fukuoka University School of Medicine.

Supported in part by a grant for cardiovascular research from the Ministry of Health and Welfare of Japan (13C-5) and a grant from the Ministry of Science, Education, and Culture of Japan (15390264).

Submitted for publication October 17, 2003; revision submitted October 29, 2003; accepted October 29, 2003.

Reprints requests: Kenji Nakayama, MD, Division of Nephrology, Endocrinology, and Vascular Medicine, Department of Medicine, Tohoku University School of Medicine, 1-1 Seiryo-Cho, Aoba-Ku, Sendai 980-8574, Japan.

0022-2143/$ – see front matter

doi:10.1016/j.jab.2003.10.012

Abbreviations: cDNA = complementary DNA; dCTP = deoxycytidine triphosphate; DMEM = Dulbecco's modified Eagle medium; EDTA = ethylenediaminetetraacetate; FCS = fetal calf serum; GAG = glycosaminoglycan; GAPDH = glyceraldehyde-3-phosphate dehydrogenase; GBM = glomerular basement membrane; GEC = glomerular epithelial cell; GMC = glomerular mesangial cell; GlcN = unsubstituted glucosamine; GlcNAc = *N*-acetylglucosamine; HEPES = *N*-2-hydroxyethylpiperazine-*N*-2-ethanesulfonic acid; HSPG = heparan sulfate proteoglycan; kb = kilobase; mRNA = messenger RNA; NDST = heparan sulfate GlcNAc *N*-deacethylase/PAPS:GlcN *N*-sulfotransferase; PAN = puromycin aminonucleoside; PAPS = adenosine 3'-phosphate 5'-phosphosulfate; PAS = periodic acid-Schiff; PBS = phosphate-buffered saline solution; PCR = polymerase chain reaction; ROS = reactive oxygen species; SDS = sodium dodecyl sulfate; SSC = standard saline citrate

Studies in both human and experimental animals indicate that the defect of size- and charge-selective barrier of the glomerular capillary wall results in the development of proteinuria, a most important and common manifestation of glomerular diseases.[1–3] Structural gaps in endothelial fenestrae, foot processes of visceral GECs, and special composition of extracellular matrix in the GBM contribute to the size-selective barrier of glomerular capillary wall.[4] The status of anionic sites in the glomerular capillary wall determines the charge-dependent selectivity.[2,5] These anionic sites are constituted by physiological anionic molecules such as HSPG in GBM and cell-surface sialoglycoproteins.[6–8] HSPG is located most densely in lamina rara interna and externa of GBM.[9] Biochemical studies suggest that sulfated portions of GAG side chains of HSPG are responsible for anionic charge in the HSPG molecule.[10–12]

It has been shown that changes in HSPG molecules, including sulfated portions in the GAG chains, are involved in the development of proteinuria in human renal diseases and in experimental models such as PAN nephrosis.[11–16] However, few studies have investigated the process that regulates sulfation of GAG chains of HSPG in the kidney. NDST is the enzyme catalyzing *N*-sulfation of unsulfated "backbone" disaccharide chains of HSPG, and the *N*-sulfation is essential for further sulfation of GAG chains.[17,18] It is possible that the disturbance of NDST is closely related to proteinuria in certain glomerular diseases, but the involvement of NDST remains to be determined.[19]

In this study, we investigated the alteration of gene expression of NDST-1, 1 of 4 isozymes of NDST,[20,21] in glomeruli in the presence of acute PAN nephrosis, a well-known experimental model of nephrotic syndrome.[22] We also studied the in vitro effect of PAN on NDST-1 mRNA expression using cultured GECs because GECs are thought to play an important role in the synthesis of HSPG in GBM.[9,23,24]

The present data indicated that NDST-1 mRNA expression is decreased with the reduction of the *N*-sulfated portion of heparan sulfate in the nephrotic state and returns to normal in the recovery state of PAN nephrosis.

METHODS

Animals. We obtained age-matched male Wistar and Sprague-Dawley rats weighing 180 to 200 g from Charles River Japan (Atsugi, Japan) and kept them in our accredited animal facilities with free access to pelleted food (Oriental Yeast Co, Ltd., Tokyo, Japan) and tap water. Animal experiments were conducted in accordance with the guidelines set forth in the National Institutes Health *Guide for the Care and Use of Laboratory Animals* (pub no 85-23).

Materials. We purchased PAN (Sigma-Aldrich, St Louis, Mo), Dulbecco's modified Eagle medium (DMEM), DMEM/Ham's F-12 medium (Gibco Laboratories, Grand Island, NY), FCS, epidermal growth factor, ITS+ premix (Collaborative Research, Inc, Bedford, Mass), OCT compound (Miles, Inc, Elkhart, Ind), phosphorus 32–labeled dCTP (NEN Research Products, Boston, Mass), a random-primed DNA-labeling kit (Boehringer Mannheim Biochemica, Mannheim, Germany), mouse monoclonal antibody against *N*-sulfated glucosamine-enriched portion of heparan sulfate (F58-10E4)[25] (Seikagaku Corp, Tokyo, Japan), fluorescein isothiocyanate–conjugated goat anti-mouse IgG + IgM antibody and goat anti-hamster IgG antibody (Jackson ImmunoResearch, West Grove, Pa) as indicated. Hamster monoclonal antibody MI90 against rat agrin,[26] a major HSPG core protein in glomeruli,[27] was provided by Professor Jo H. M. Berden (Department of Nephrology, Nijmegen University Hospital, Nijmegen, The Netherlands).

A 2.4-kb cDNA probe specific for rat NDST-1[28] and a 1.3-kb cDNA probe specific for GAPDH[29] were prepared from the plasmids provided by Dr Carlos B. Hirschberg (Department of Biochemistry and Molecular Biology, University of Massachusetts Medical Center, Worcester, Mass) and Dr Ph. Fort (Institut de Génétique Moléculaire, Université Montpellier, Montpellier, France), respectively.

Animal model. We divided 20 Wistar rats into 2 groups of 10 rats each. In 1 group, PAN nephrosis was induced with an intraperitoneal injection of 150 mg/kg PAN dissolved in 2 mL of saline solution.[30] Rats in the other group were injected with saline solution alone and used as controls. Five rats in each group were killed under diethyl ether anesthesia on days 10 and 35. These time points were chosen because previous studies had shown that massive proteinuria developed by day 10 and disappeared by day 35 after the single 150 mg/kg

injection of PAN.[30] Immediately after animals were killed, the kidneys were processed for histological study and Northern-blot analysis as described below. The entire experiment was repeated 3 times independently.

Twenty-four-hour urine and blood samples were collected from each rat before it was killed. Urinary protein was determined as daily excretion in 24-hour urine with the use of the Biuret method as reported previously.[31] Serum concentrations of albumin, creatinine, and total cholesterol were measured with a Synchron CX3 chemical analyzer (Beckman, Tokyo, Japan) or Dri-Chem 5000 analyzer (Fuji Film, Tokyo, Japan).

Histologic studies. For light microscopy, renal tissue was fixed in 95% ethanol for 24 hours at 4°C and embedded in paraffin as described previously.[32] Two-micrometer sections were stained with PAS or periodic acid methenamine silver in accordance with conventional methods. For electron microscopy, we fixed blocks (1.5 mm^3) of renal tissue in 2.5% glutaraldehyde and 2% paraformaldehyde followed by postfixation with 1% osmium tetroxide. The blocks were then dehydrated and embedded in Epon 812 (TAAB Laboratories Equipment Ltd., Aldermaston, Berkshire, England). Ultrathin sections (60 nm) were mounted on coated copper grids, stained with uranyl acetate and lead citrate, and then examined with a JEOL 1010 electron microscope (Nippon Denshi, Tokyo, Japan).[33]

For immunohistochemistry, we embedded renal tissue in OCT compound, snap-froze it in precooled hexane, and stored it in liquid nitrogen until use. Four-micrometer cryostat sections were air-dried and fixed in acetone for 10 minutes at room temperature. *N*-sulfated portions of GAG chains in HSPG and agrin were detected with the use of a standard immunofluorescence method with monoclonal antibodies F58-10E4[25] and anti-agrin MI90,[26] respectively. In brief, the specimens were incubated with the antibodies diluted in PBS at a ratio of 1:100 for 1 hour at 37°C. After 3 washes with PBS, the specimens were further incubated with fluorescein isothiocyanate–goat anti-mouse IgG + IgM antibody or goat anti-hamster IgG antibody (Jackson) diluted in PBS at a ratio of 1:100 for 1 hour at 37°C. They were washed again with PBS, then examined under a BH2 RFL T2 fluorescence microscope (Olympus Optical Co, Ltd, Tokyo, Japan). Photographs were taken with a PM-10AD automatic timer (Olympus). Two of the authors independently examined the kidney sections and scored the intensity of staining for 10E4 and agrin in GBM of each glomerulus semiquantitatively, using an arbitrary scale of 4 grades (0–3), depending on the degree of staining intensity. The mean and SD in all groups of 5 rats were calculated, with an average score of 30 glomeruli for each rat specimen.

Cell culture. GECs isolated from Sprague-Dawley rats were provided by Dr Hideaki Yamabe (Second Department of Internal Medicine, Hirosaki University School of Medicine, Hirosaki, Japan).[34,35] GECs were cultured in plates coated with collagen type I in DMEM-H containing 5% FCS, 2 mmol/L L-glutamine, 10 ng/mL epithelial growth factor, and 1% ITS+ premix.[36] GMCs were isolated from Sprague-Dawley rats and maintained in DMEM containing 10% FCS, 2 mmol/L L-glutamine and 1% ITS+ premix as described previously.[29]

For experiments, confluent GECs were washed 3 times with DMEM-H containing 0.5% FCS and incubated with DMEM-H containing 0.5% FCS in the absence or the presence of PAN at various concentrations (5–500 ng/mL). Confluent GMCs were washed and treated in the same manner with DMEM containing 0.5% FCS. After incubation, cells were washed 3 times with PBS, frozen with liquid nitrogen, and stored at −80°C until use for RNA isolation. After incubation of GECs with PAN, cell viability was determined with the use of the trypan blue exclusion test.

RNA isolation and Northern-blot analyses. On days 10 and 35 after injection of PAN or saline solution, we isolated glomeruli from the kidneys using the sequential-sieving method.[37] The glomeruli from 5 rats in each group were pooled, and total RNA was isolated from the pooled glomeruli with the use of the acid-guanidium-phenol-chloroform method.[38] Cellular RNA was also isolated from cultured GECs and GMCs. After determining the amount of RNA with a spectrophotometer, we applied 30 μg of each RNA to 1.0% agarose gel containing 2.2 mol/L formaldehyde, subjected the gels to electrophoresis for 4 hours at 100 V and blotted them to nitrocellulose membrane. Prehybridization and hybridization were performed in a solution containing 50% formaldehyde, 50 mmol/L HEPES-KOH (pH 7.3), 1 mmol/L EDTA, 0.2% SDS, 3× SSC, and 5× Denhart's solution. After 2 hours of prehybridization at 42°C with 200 μg/mL of denatured salmon-sperm DNA, hybridization was performed at 42°C overnight with cDNA for rat NDST-1 radiolabeled with [32P]dCTP. After hybridization, the blot was washed extensively with 1× SSC–0.1% SDS at 42°C for 20 minutes and then 1× SSC - 0.1% SDS at 68°C three times for 20 minutes each. Control hybridization was performed with cDNA for rat GAPDH. Autoradiography to detect NDST-1 mRNA and GAPDH mRNA, respectively, was performed for 24 or 6 hours at room temperature with a BAS Imaging Plate (Fuji Film). Expression of each mRNA was measured quantitatively with the BAS-2000 system (Fuji Film), and the expression of NDST-1 mRNA was calculated as a relative ratio against that of GAPDH mRNA. The results were expressed as a percentage of the ratio relative to those in control.

Real-time PCR. For the quantitative measurement of NDST-1 mRNA levels in GMC, we performed real-time polymerase chain reaction using the ABI PRISM 7700 Sequence Detector and TaqMan Predeveloped Assay Reagents for the Gene Expression Quantification System (Applied Biosystems, Foster City, Calif). Using multiple reporter dyes, we assayed the mRNA levels of NDST-1 and endogenous control (GAPDH). NDST-1 mRNA levels were expressed as the ratio relative to the endogenous control. The sequence of the probes were as follows: forward primer sequence, ACTCATATTGAACGCTGGCTCA; reverse primer sequence, TCTGCACTGTGTCCATCACTTTG; TaqMan probe sequence, CATGCCAACCAGATCCTGGTCTTGGAT.

Statistical analysis. All values are expressed as mean ± SD. Data were analyzed with the use of Student's *t* test for unpaired samples or the Spearman rank-correlation coefficient. *P* values of less than .05 were considered statistically significant.

Table I. Summary of blood and urine analyses

Treatment group	Urinary protein (mg/day)	Albumin (g/dL)	Cholesterol (mg/dL)	Creatinine (mg/dL)
PAN				
Day 10	853.9 ± 152.0*	0.78 ± 0.13*	353.3 ± 20.0*	0.35 ± 0.06
Day 35	53.0 ± 32.7	3.55 ± 0.13	95.0 ± 2.7	0.33 ± 0.05
Saline solution				
day 10	21.6 ± 2.2	3.02 ± 0.08	115.2 ± 5.5	0.36 ± 0.05
day 35	27.7 ± 12.3	3.45 ± 0.13	82.8 ± 4.7	0.43 ± 0.05

Data expressed as the mean ± SD (n = 5).
*$P < .05$ vs controls at each time point.

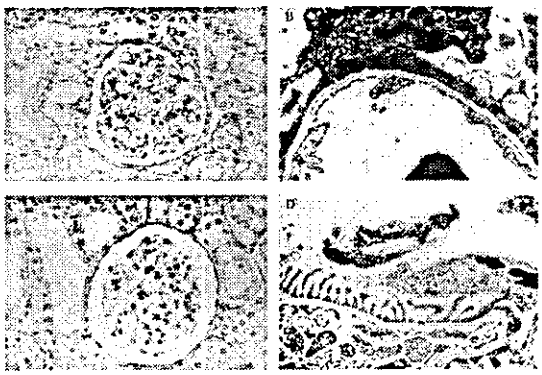

Fig 1. Representative photographs of renal histology under light microscopy (*A* and *C*, PAS staining, original magnification 200×) and electron microscopy (*B* and *D*, original magnification 16,000×). On day 10 after injection of PAN we detected no apparent changes under light microscopy (**A**) and effacement of foot processes of GECs under electron microscopy (**B**). We noted no abnormalities in histology on day 35 in PAN-treated rats (**C** and **D**).

RESULTS

Clinical and histological analyses of PAN nephrosis. On day 10, PAN-treated rats exhibited massive proteinuria, decreased serum albumin, and increased serum cholesterol (Table I). On day 35, these parameters were not significantly different between PAN-treated rats and controls. We detected no significant changes in serum creatinine in PAN-treated rats compared with that in controls.

No obvious macroscopic changes (Fig 1, *A*) but foot-process effacement on electron microscopy (Fig 1, *B*) of visceral GECs were observed on day 10 in PAN-treated rats. We detected no structural abnormalities on day 35 in the glomeruli of PAN-treated rats on light and electron microscopy (Fig 1, *C* and *D*).

Expression of NDST-1 mRNA in PAN nephrosis. To examine the expression of NDST-1 mRNA in pooled glomeruli, we performed Northern blotting. Glomerular expression of NDST-1 mRNA was observed as a single transcript of 8.5 kb. In PAN-treated rats, the expression of NDST-1 mRNA was reduced on day 10 (Fig 2, *A*). Densitometric analyses of the autoradiographs from 3 independent series of experiments showed that the ratios of NDST-1 mRNA against GAPDH mRNA in PAN-treated rats were significantly decreased, to 48% ± 6% of those in controls (Fig 2, *B*). On day 35, the expression of NDST-1 mRNA in the glomeruli of PAN-treated rats was 85% ± 10% of those in controls (Fig 2, *C* and *D*).

Immunofluorescence studies. Because Northern-blot analysis and examination of urine and blood as described above indicated that the decrease in expression of NDST-1 mRNA was correlated with the appearance of significant proteinuria, we sought to determine whether changes of *N*-sulfation of GAG chains occurred in the kidney. Frozen sections of renal tissue were analyzed under immunofluorecence microscopy with the specific antibody against *N*-sulfated glucosamine–enriched portion of heparan sulfate, 10E4.[25] Control rats showed well-stained GBM, Bowman's capsule, and tubular basement membrane (Fig 3, *B*), consistent with the earlier report.[25] In PAN-treated rats, we detected a significant decrease in staining in GBM on day 10, whereas the intensity of staining was not changed in other parts of the renal sections, including Bowman's capsule and tubular basement membrane (Fig 3, *A*). When we analyzed the sections with the antibody against agrin,[26] staining intensity was not changed in either group on day 10 (Fig 3, *C* and *D*). On day 35, PAN-treated rats showed intensity of staining of 10E4 on GBM similar to that in controls (data not shown). Semiquantitative analysis of staining intensity in GBM showed significant decrease of *N*-sulfated portion of heparan sulfate in PAN-treated rat GBM on day 10 compared with those in the saline solution–treated control (1.48 ± 0.11 vs 2.68 ± 0.13, $P < .05$; Table II).

Expression of NDST-1 mRNA in cultured GECs and GMCs. To further investigate the decrease in the glomerular expression of NDST-1 mRNA in PAN nephrosis rats, we studied the expression of NDST-1 mRNA in cultured GECs and GMCs. The expression of NDST-1 mRNA was 2.7 times greater in GECs than in GMCs in cells cultured for 24 hours with medium alone ($n = 3$; Fig 4).

In the next set of experiments, we studied the effect

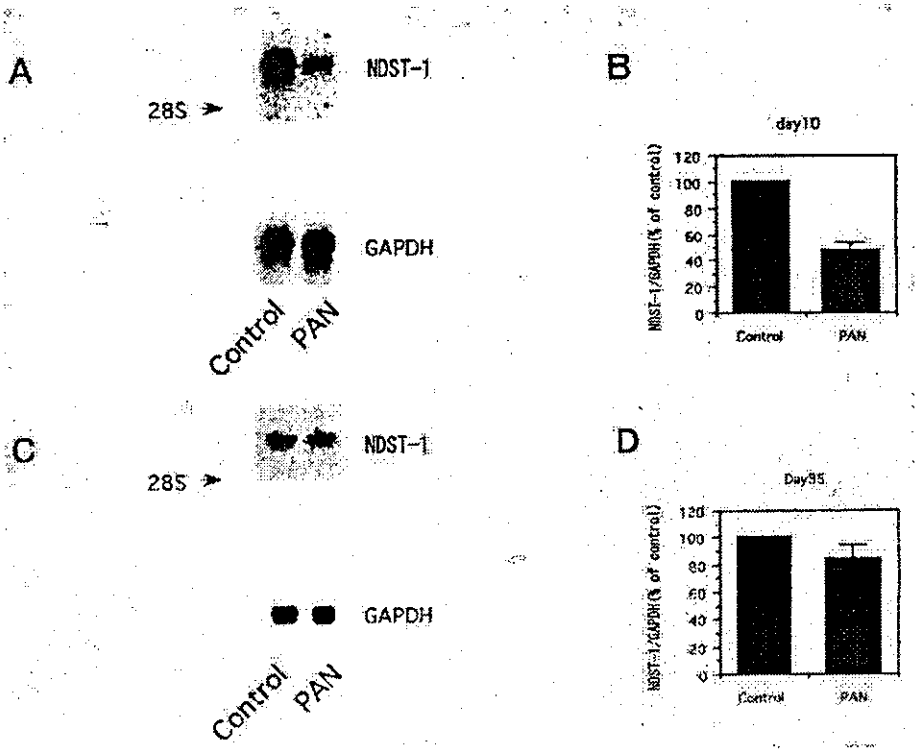

Fig 2. Northern-blot analysis for glomerular expression of NDST-1 mRNA. Northern blotting was performed with total RNA isolated on (**A**) day 10 or (**C**) day 35 from the glomeruli of PAN-treated rats or rats injected with saline solution alone. Specific probes for rat NDST-1 or GAPDH were used as described in the Methods. Densitometric analysis showed the decrease in expression of NDST-1 mRNA on day 10 in PAN-treated rats compared with that in rats injected with saline solution alone (**B**). Only minor differences in the expression of NDST-1 mRNA were observed on day 35 between PAN-treated rats and rats injected with saline solution alone (**D**). The ratio of NDST-1 mRNA against GAPDH mRNA in controls is denoted by 100%. Data expressed as mean ± SD of 3 independent experiments.

of PAN on the expression of NDST-1 mRNA by cultured GECs. Incubation of GECs for 24 hours in the presence of 50 ng/mL PAN resulted in a significant decrease in the expression of NDST-1 mRNA compared with that in controls ($n = 3$; Fig 5). Densitometric analysis revealed that the ratio of the expression of NDST-1 mRNA against GAPDH mRNA in GECs incubated for 24 hours in the presence of PAN was 67% ± 12% of that in controls ($P < .05$). The ratio in GECs cultured for 3 hours with 50 ng/mL PAN was 89% ± 17% of those in controls. GECs incubated for 24 hours with medium alone showed an increase in expression of NDST-1 mRNA compared with that in cells incubated for 3 hours with medium (Fig 5). In dose-response experiments, GECs were incubated for 24 hours with different concentrations of PAN. The expression of NDST-1 mRNA in GECs decreased significantly in a dose-dependent manner ($n = 3$; Fig 6). GEC death was not observed in this range during the experiments.

Because GMCs expressed less NDST-1 mRNA than did GECs, we performed real-time PCR to assess NDST-1 mRNA levels in GMCs. In contrast with GECs, GMCs incubated with PAN for 24 hours showed no significant decrease in the expression of NDST-1 mRNA ($n = 3$; Fig 7).

DISCUSSION

The findings of previous studies have indicated that the anionic charge in GBM is located predominantly in sulfate groups of GAG chains in HSPG.[12,39] *N*-sulfation catalyzed by NDSTs is the first and essential step in the enzymatic reactions for the sulfations of heparan sulfate GAG chain.[17,18,40,41]

Recently some heparan sulfate sulfotransferases, including 4 isozymes of NDST and 2-,3-,6-O-sulfotransferases were cloned.[20,21,28,42–45] NDST is a key enzyme that plays a pivotal role in the sulfation pathway in heparan sulfate GAG chain synthesis. Isozymes of NDST, NDST-1 (rat liver),[28] NDST-2 (murine mastocytoma),[42] NDST-3 (human brain),[20] and NDST-4 (hu-

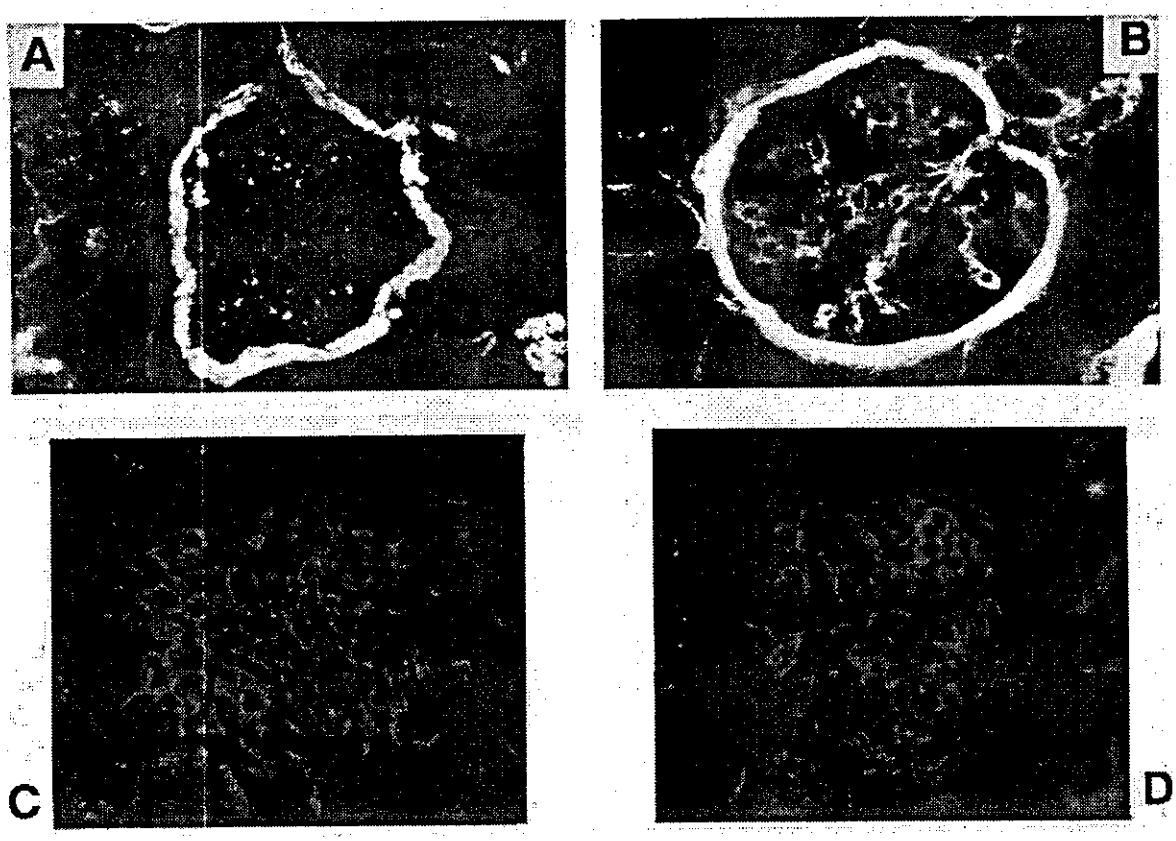

Fig 3. Immunohistochemical studies. We detected *N*-sulfated glucosamine-enriched portions of heparan sulfate and core protein agrin on frozen sections of renal tissues using specific antibodies — F58-10E4 (**A** and **B**) and MI90 (**C** and **D**), respectively (original magnification 200×). On day 10 after injection of saline solution (*B*), staining of GBM, Bowman's capsule, and tubular basement membrane by 10E4 was clear. In PAN-treated rats (*A*), the staining intensity of 10E4 on GBM was apparently decreased on day 10. We detected no differences in staining by M190 on day 10 in PAN-treated rats (*C*) and rats injected with saline solution (*D*).

Table II. Semiquantitative analysis of immunofluorescence staining

Treatment group	*N*-sulfated portion of heparan sulfate (10E4)	Agrin (MI90)
PAN		
Day 10	1.48 ± 0.11*	1.61 ± 0.36
Day 35	2.46 ± 0.15	ND
Saline solution		
Day 10	2.68 ± 0.13	1.67 ± 0.25
Day 35	2.58 ± 0.15	ND

The intensity of staining for 10E4 and agrin in GBM of each glomerulus was scored semiquantitatively, as described in the Methods section.
Data expressed as mean ± SD (n = 5).
*$P < .05$ vs controls at each time point. *ND* = not determined.

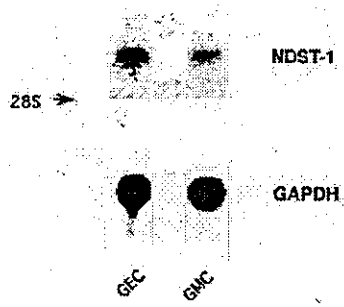

Fig 4. Expression of NDST-1 mRNA in cultured GECs and GMCs. Northern-blot analysis was performed with total RNA isolated from the cells incubated for 24 hours with the media as described in the Methods.

man and mouse cDNA library)[21] have been identified, but their distribution and relative contribution in heparan sulfate synthesis in certain tissues are largely unknown. Aikawa and Esko[20,21] reported that NDST-1, -2, and -3 are expressed in human kidney, but the contribution of each isozyme to heparan sulfate sulfa-

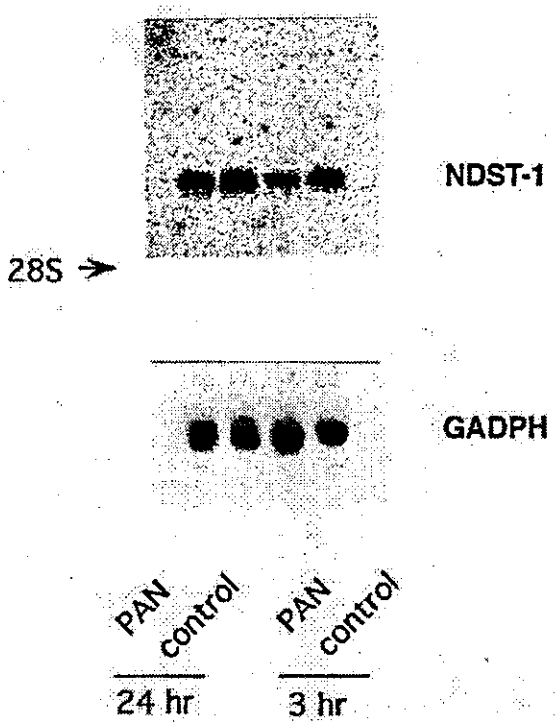

Fig 5. Effect of PAN on expression of NDST-1 mRNA in cultured GECs. Northern-blot analysis was performed with total RNA isolated from GECs incubated for 3 or 24 hours in the presence of 50 ng/mL PAN as described in the Methods section.

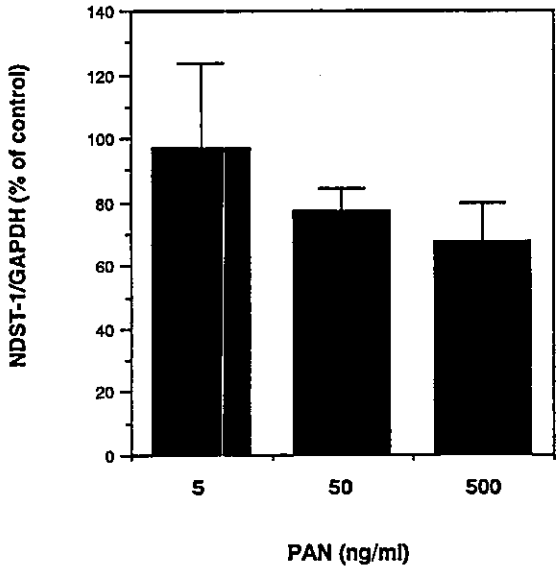

Fig 6. Summary of Northern-blot analyses in dose-response experiments in GECs. GECs were incubated for 24 hours in the presence of PAN at concentrations of 5, 50, and 500 ng/mL. The percentages of the ratio of NDST-1 mRNA expression were calculated relative to the ratio in controls as described in the Methods. The ratio of the expression of NDST-1 mRNA against GAPDH mRNA in controls is indicated by 100%. Data expressed as mean ± SD of 3 independent experiments.

tion in the glomeruli remains to be elucidated. Our data suggest that NDST-1 activity is involved in the sulfation of HS in glomeruli, consistent with a recent report in NDST-1–knockout mice.[46]

In this study, we demonstrated that glomerular expression of NDST-1 mRNA in PAN-treated rats was decreased at the nephrotic phase. The reduction in the level of NDST-1 mRNA was accompanied by a loss of *N*-sulfated GAG chains of HSPG in GBM without changes in core protein agrin, suggesting a decrease in NDST activity. Furthermore, the disappearance of significant proteinuria corresponded with the return to normal expression of NDST-1 mRNA in glomeruli and of *N*-sulfated GAG chains in GBM.

These results indicate that a disturbance of enzymatic reaction for sulfations in GAG chains of HSPG plays an important role in the mechanism of significant proteinuria in the PAN nephrosis model; the authors of recent studies have reported that changes in cell-surface sialoglycoproteins (eg, podocalyxin and podoplanin) or foot process–associated molecules (including nephrin and podocin on podocytes) are also involved in the development of proteinuria in this animal model.[47–49] Furthermore, our results are consistent with those from other studies demonstrating that the injection of specific antibodies against the heparan sulfate GAG side chain of HSPG induces proteinuria, probably by masking anionic charge in the heparan sulfate GAG side chain,[14] whereas antibodies against the core protein of HSPG do not cause proteinuria.[50]

In this study, the changes in glomerular expression of NDST-1 and *N*-sulfated GAG chains were assessed at a limited number of time points. To determine clearly the causality of alterations of the heparan sulfate sulfation pathway to proteinuria in PAN nephrosis, further investigation at multiple time points, especially earlier ones, is needed.

Several reports suggest a role for ROS in PAN nephrosis.[51,52] Raats and Berden[19] reported that heparan sulfate side chains of rat agrin were depolymerized in vitro by ROS and suggest that ROS can affect the permeability of the GBM by way of heparan sulfate depolymerization. It may be that the decrease in NDST-1 in glomeruli impaired the repair process for the heparan sulfate initially damaged by ROS in GBM, leading to massive proteinuria.

We also demonstrated in this study that GECs expressed more NDST-1 mRNA than GMCs, a finding in agreement with the results of recent in vitro studies showing that GECs synthesize more HSPG than do

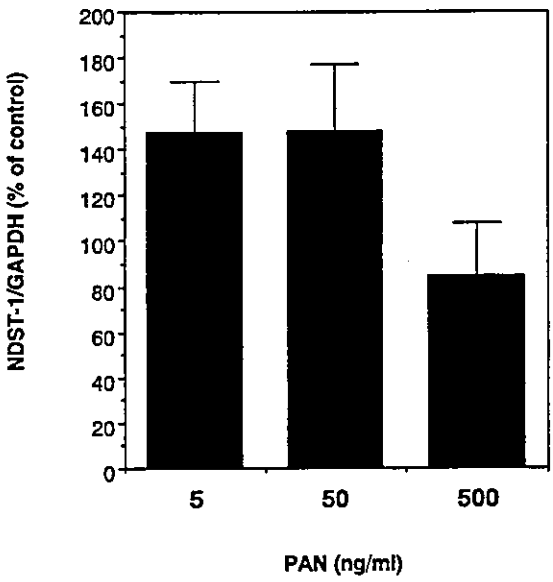

Fig 7. Summary of real-time PCR in dose-response experiments in GMCs. GMCs were incubated for 24 hours in the presence of PAN at concentrations of 5, 50, and 500 ng/mL. The percentages of the ratio of NDST-1 mRNA expression were calculated relative to the ratio in controls as described in the Methods section. The ratio of the expression of NDST-1 mRNA against GAPDH mRNA in controls is denoted by 100%. Data expressed as mean ± SD of 3 independent experiments.

GMCs as detected on ELISA with a specific antibody against heparan sulfate GAG side chain in HSPG.[53] The incubation of GECs with PAN reduces the expression of NDST-1 mRNA in a time- and dose-dependent manner. We used PAN in culture at concentrations ranging from 5 to 500 ng/mL; no GEC death was observed in this range during the experiments. It has been shown that the concentration of PAN capable of inducing general toxicity is at least 10 μg/mL.[34,54] In addition, the production of the core protein of HSPG in GECs is known to be unaltered in the presence of PAN at a concentration less than 50 μg/mL.[55] Thus the results showed that NDST-1 is involved in the assembly of heparan sulfate in GEC, and suggests that GECs, rather than GMCs, contribute to the glomerular disturbance of *N*-sulfation of heparan sulfate after administration of PAN, without the change of HSPG core protein, including agrin.

Taken together, our results show for the first time, to our knowledge, that transcriptional alteration of the glomerular NDST-1 occurs at a nephrotic phase in PAN nephrosis. We suggest that the alteration of NDST-1 mRNA in glomeruli is associated with the reduction of *N*-sulfated GAG chains of HSPG on GBM and contributes at least somewhat to the mechanism of proteinuria in the PAN nephrosis model. Because a previous report indicated that GEC is the major target of PAN in PAN nephrosis,[56] it may be that the transcriptional decrease of NDST-1 in GEC contributes to the undersulfation of heparan sulfate in GBM and proteinuria in PAN nephrosis.

We thank Professor Mohamed R. Daha, Professor Leendert A. van Es and Dr Emile de Heer for their critical review of this paper.

REFERENCES

1. Chang RLS, Deen WM, Robertson CR, Brenner BM. Permselectivity of the glomerular capillary wall. III. Restricted transport of polyanions. Kidney Int 1975;8:212–8.
2. Brenner BM, Hostetter TH, Humes HD. Molecular basis of proteinuria of glomerular origin. N Engl J Med 1978;298:826-833.
3. Guasch A, Deen WM, Myers BD. Charge selectivity of the glomerular filtration barrier in healthy and nephrotic humans. J Clin Invest 1993;92:2274-82.
4. Kanwar YS. Biophysiology of glomerular filtration and proteinuria. Lab Invest 1984;51:7-21.
5. Remuzzi A, Remuzzi G. Glomerular perm-selective function. Kidney Int 1994;45:398-402.
6. Kitano Y, Yoshikawa N, Nakamura H. Glomerular anionic sites in minimal change nephrotic syndrome and focal segmental glomerulosclerosis. Clin Nephrol 1993;40:199-204.
7. Kanwar YS, Farquhar MG. Presence of heparan sulfate in the glomerular basement membrane. Proc Natl Acad Sci U S A 1979;76:1303-7.
8. Kerjaschki D, Sharkey DJ, Farquhar MG. Identification and characterization of podocalyxin — the major sialoprotein of the renal glomerular epithelial cell. J Cell Biol 1984;98:1591-8.
9. Stow JL, Sawada H, Farquhar MG. Basement membrane heparan sulfate proteoglycans are concentrated in the lamina rarae and in podocytes of the rat renal glomerulus. Proc Natl Acad Sci U S A 1985;82:3296-300.
10. Kanwar YS, Linker A, Farquhar MG. Increased permeability of the glomerular basement membrane to ferritin after removal of glycosaminoglycans (heparan sulfate) by enzyme digestion. J Cell Biol 1980;86:688-93.
11. Tamsma JT, van den Born J, Bruijn JA, Assmann KJM, Weening JJ, Berden JHM, et al. Expression of glomerular extracellular matrix components in human diabetic nephropathy: decrease of heparan sulfate in the glomerular basement membrane. Diabetologia 1994;37:313-20.
12. van der Woude FJ, van Det NF. Heparan sulfate proteoglycans and diabetic nephropathy. Exp Nephrol 1997;5:180-8.
13. van den Born J, van den Heuvel LPWJ, Bakker MAH, Veerkamp JH, Assmann KJM, Weening JJ, et al. Distribution of GBM heparan sulfate proteoglycan core protein and side chains in human glomerular diseases. Kidney Int 1987;43:454-63.
14. van den Born J, van den Heuvel LPWJ, Bakker MAH, Veerkamp JH, Assmann KJM, Berden JHM. A monoclonal antibody against GBM heparan sulfate induces an acute selective proteinuria in rats. Kidney Int 1992;41:115-23.
15. Caulfield JP, Farquhar MG. Loss of anionic sites from the glomerular basement membrane in aminonucleoside nephrosis. Lab Invest 1978;39:505-12.
16. Olson JL, Rennke HG, Venkatachalam MA. Alterations in the charge and size selectivity barrier of the glomerular filter in aminonucleoside nephrosis in rats. Lab Invest 1981;44:271-9.
17. Brandan E, Hirschberg CB. Purification of rat liver *N*-heparan sulfate sulfotransferase. J Biol Chem 1988;263:2417-22.
18. Bame KJ, Esko JD. Undersulfated heparan sulfate in a Chinese hamster ovary cell mutant defective in heparan sulfate *N*-sulfotransferase. J Biol Chem 1989;264:8059-65.

19. Raats CJI, van den Born J, Berden JHM. Glomerular heparan sulfate alterations: mechanisms and relevance for proteinuria. Kidney Int 2000;57:385-400.
20. Aikawa J, Esko JD. Molecular cloning and expression of a third member of the heparan sulfate/heparin GlcNAc *N*-deacetylase/*N*-sulfotransferase family. J Biol Chem 1999;274:2690-5.
21. Aikawa J, Grobe K, Tsujimoto M, Esko JD. Multiple isozymes of heparan sulfate/heparin GlcNAc N-deacetylase/GlcN N-sulfotransferase. Structure and activity of the fourth member, NDST4. J Biol Chem 2001;276:5876-82.
22. Frenk S, Antonowicz I, Craig JM, Metcoff J. Experimental nephrotic syndrome induced in rats by aminonucleoside. Renal lesion and body electrolyte composition. Proc Soc Exp Biol Med 1955;89:424-7.
23. Striker GE, Killen PD, Farin FM. Human glomerular cells in vitro: isolation and characterization. Transplant Proc 1980;12:88-99.
24. Lee LK, Pollock AS, Lovett DH. Asymmetric origins of the mature glomerular basement membrane. J Cell Physiol 1993;157:169-77.
25. David G, Bai XM, van der Schueren B, Cassiman JJ, van den Berghe H. Developmental changes in heparan sulfate expression: in situ detection with mAbs. J Cell Biol 1992;119:961-75.
26. Raats CJI, Bakker MAH, Hoch W, Tamboer WPM, Groffen AJA, van den Heuvel LPWJ, et al. Differential expression of agrin in renal basement membranes as revealed by domain-specific antibodies. J Biol Chem 1998;273:17832-8.
27. Groffen AJ, Ruegg MA, Dijkman HBPM, van den Verden TJ, Buskens CA, van den Born J, et al. Agrin is a major heparan sulfate proteoglycan in the human glomerular basement membrane. J Histochem Cytechem 1998;46:19-27.
28. Hashimoto Y, Orellana A, Gil G, Hirschberg CB. Molecular cloning and expression of rat liver *N*-heparan sulfate sulfotransferase. J Biol Chem 1992;267:15744-50.
29. Fort Ph, Marty L, Piechaczyk H, El Sabrouty S, Dani C, Jeanteur Ph, et al. Various rat adult tissues express only one major mRNA species from the glyceraldehyde-3-phosphate dehydrogenase multigenic family. Nucleic Acids Res 1985;13:1431-42.
30. Natori Y, Igawa Y, Nakao N, Natori Y. Cytotoxicity of sera from rats with puromycin aminonucleoside nephrosis. Nephron 1996; 73:258-63.
31. Natori Y, Hayakawa I, Shibata S. Passive Heymann nephritis with acute and severe proteinuria induced by heterologous antibody against renal tubular brush border glycoprotein gp108. Lab Invest 1986;55:63-70.
32. Ootaka T, Suzuki M, Sudo K, Sato H, Seino J, Saito T, et al. Histologic localization of terminal complement complexes in renal diseases. Am J Clin Pathol 1989;91:144-51.
33. Sato H, Saito T, Seino J, Ootaka T, Kyogoku Y, Furuyama T, et al. Dense deposit disease, its possible pathogenesis suggested by an observation of a patient. Clin Nephrol 1987;27:41-5.
34. Yamabe H, Yoshikawa S, Ohsawa H, Inuma H, Miyata M, Sasaki T, et al. Tissue factor production by cultured rat glomerular epithelial cells. Nephrol Dial Transplant 1993;8:519-23.
35. Natori Y, Natori Y, Nishimura T, Yamabe H, Iyonaga K, Takeya M, et al. Production of monocyte chemoattractant protein-1 by cultured glomerular epithelial cells: inhibition by dexamethasone. Exp Nephrol 1997;5:318-22.
36. Natori Y, O'Meara YM, Manning EC, Minto AWM, Levine JS, Weise WJ, et al. Production and polarized secretion of basement membrane components by glomerular epithelial cells. Am J Physiol 1992;262:F131-7.
37. Harper CA, Robinson JM, Hoover RL, Wright TC, Karnovsky MJ. Improved methods for culturing rat glomerular cells. Kidney Int 1984;26:875-80.
38. Chomczynski P, Sacchi N. Single step method of RNA isolation by acid–guanidine thiocyanate–phenol–chloroform extraction. Anal Biochem 1987;162:156-9.
39. Kjellen L, Lindahl U. Proteoglycan: structure and interactions. Annu Rev Biochem 1991;60:443-75.
40. Ishihara M, Guo Y, Wei Z, Yang Z, Swiedler SJ, Orellana A, et al. Regulation of biosynthesis of the basic fibroblast growth factor binding domains of heparan sulfate by heparan sulfate-*N*-deacetylase/*N*-sulfotransferase expression. J Biol Chem 1993;268:20091-5.
41. Lindahl U, Lidholt K, Spillmann D, Kjellen L. More to "heparin" than anticoagulation. Thrombosis Res 1994;75:1-32.
42. Orellana A, Hirschberg CB, Wei Z, Swiedler SJ, Ishihara M. Molecular cloning and expression of a glycosaminoglycan *N*-acetylglucosaminyl *N*-deacethylase/*N*-sulfotransferase from a heparin-producing cell line. J Biol Chem 1994;269:2270-6.
43. Shworak NW, Liu J, Fritze LM, Schwartz JJ, Zhang L, Logeart D, et al. Molecular cloning and expression of mouse and human cDNAs encoding heparan-sulfate D-glucosaminyl 3-O-sulfotransferase. J Biol Chem 1997;272:28008-19.
44. Habuchi H, Kobayashi M, Kimata K. Molecular characterization and expression of heparan-sulfate 6-sulfotransferase. Complete cDNA cloning in human and partial cloning in Chinese hamster ovary cells. J Biol Chem 1998;273:9208-13.
45. Kobayashi M, Habuchi H, Yoneda M, Habuchi O, Kimata K. Molecular cloning and expression of Chinese hamster ovary cell heparan-sulfate 2-sulfotransferase. J Biol Chem 1997;272:13980-5.
46. Ringvall M, Ledin J, Holmborn K, van Kuppevelt T, Ellin F, Eriksson I, et al. Defective heparan sulfate biosynthesis and neonatal lethality in mice lacking *N*-deacetylase/*N*-sulfotransferase-1. J Biol Chem 2000;275:25926-30.
47. Kerjaschki D, Vernillo AT, Farquhar MG. Reduced sialylation of podocalyxin — the major sialoprotein of the rat kidney glomerulus — in aminonucleoside nephrosis. Am J Pathol 1985;118:343-9.
48. Breiteneder-Geleff S, Matsui K, Soleiman A, Meraner P, Poczewski H, Kalt R, et al. Podoplanin, novel 43-kd membrane protein of glomerular epithelial cells, is down-regulated in puromycin nephrosis. Am J Pathol 1997;151:1141-52.
49. Kawachi H, Koike H, Kurihara H, Yaoita E, Orikasa M, Shia MA, et al. Cloning of rat nephrin: expression in developing glomeruli and in proteinuric states. Kidney Int 2000;57:1949-61.
50. Makino H, Gibbons JT, Kumudavalli Reddy M, Kanwar YS. Nephritogenicity of antibodies to proteoglycans of the glomerular basement membrane-1. J Clin Invest 1986;77:142-56.
51. Diamond JR, Bonventre JV, Karnovsky MJ. A role for oxygen free radicals in aminonucleoside nephrosis. Kidney Int 1986;29:478-83.
52. Gwinner W, Landmesser U, Brandes RP, Kubat B, Plasger J, Eberhard O, et al. Reactive oxygen species and antioxidant defense in puromycin aminonucleoside glomerulopathy. J Am Soc Nephrol 1997;8:1722-31.
53. van Det NF, van den Born J, Tamsma JT, Verhagen NAM, van den Heuvel LPWJ, Berden JHM, et al. Proteoglycan production by human glomerular visceral epithelial cells and mesangial cells in vitro. Biochem J 1995;307:759-68.
54. Fishman JA, Karnovsky MJ. Effects of the aminonucleoside of puromycin on glomerular epithelial cells in vitro. Am J Pathol 1985;118:398-407.
55. Kasinath BS, Singh A, Kanwar YS, Lewis EJ. Effect of puromycin aminonucleoside on HSPG core protein content of glomerular epithelial cells. Am J Physiol 1988;255:F590-6.
56. Ryan GB, Karnovsky MJ. An ultrastructural study of the mechanisms of proteinuria in aminonucleoside nephrosis. Kidney Int 1975;8:219-32.

J Am Soc Nephrol 15: 276–285, 2004

Activation of the Signal Transducer and Activator of Transcription Signaling Pathway in Renal Proximal Tubular Cells by Albumin

HIDEAKI NAKAJIMA,* MASARU TAKENAKA,*‡ JUN-YA KAIMORI,* TAKAYUKI HAMANO,* HIROTSUGU IWATANI,* TAKESHI SUGAYA,† TAKAHITO ITO,* MASATSUGU HORI,* and ENYU IMAI*

**Department of Internal Medicine and Therapeutics, Osaka University Graduate School of Medicine, Osaka, †Center of Tsukuba Advanced Research Alliance, Institute of Applied Biochemistry, University of Tsukuba, Ibaraki, and ‡Graduate School of Life Science, Kobe Women's University, Kobe, Japan.*

Abstract. Renal proximal tubular cells activated by reabsorption of protein are thought to play significant roles in the progression of kidney diseases. It was hypothesized that the signal transducer and activator of transcription (STAT) proteins may be activated by proteinuria in proximal tubular cells. To test this hypothesis, murine proximal tubular cells were treated with albumin (30 mg/ml medium) for various lengths of time. The results showed that albumin could activate Stat1 and Stat5 within 15 min in proximal tubular cells. The activation of STATs was mediated mostly by Jak2 and required no protein synthesis. In addition, activation of Stat1 occurred even after neutralization of IFN-γ. The activation of STATs was inhibited by *N*-acetyl-L-cysteine, a precursor of glutathione and a reactive oxygen species (ROS) scavenger, and fluorescence-activated cell sorter analysis showed upregulation of intracellular ROS after albumin overloading, suggesting that albumin *per se* could generate ROS in proximal tubular cells. The activation of STATs occurred by way of the ROS generating system, and especially through the membrane-bound NADPH oxidase system. Reduced activities of glutathione peroxidase and catalase could also be responsible for the accumulation of intracellular ROS. Hence, not only the ROS generating system, but also the ROS scavenging system may contribute to the induction of ROS by albumin. These findings support the hypothesis that proximal tubular cells are activated and generate ROS by reabsorption of abundant urinary proteins filtered through the glomerular capillaries, and as a consequence, various IFN-γ–inducible proteins are synthesized through IFN-γ–independent activation of STAT signaling.

Janus kinase (JAK) and the signal transducer and activator of transcription (STAT) proteins were originally defined largely in the context of interferon (IFN) signaling (1–3). The JAK/STAT signaling pathway was also first defined in the same context. A total of seven different STAT family members (Stat1, Stat2, Stat3, Stat4, Stat5a, Stat5b, and Stat6) have now been identified in mammalian cells (4), and a large number of cytokines, growth factors, reactive oxygen species (ROS), and others are now known to trigger STAT activation (5–7). The fundamental roles of STATs in highly diverse biologic processes have been identified by using STAT knockout mice and/or by tissue-specific deletions (8,9). These processes include innate and adaptive immune function, embryonic development, cell differentiation, cell proliferation, survival, and apoptosis (10–14), and the STAT family has become a therapeutic target in human cancer (15).

Renal proximal tubular cells play central roles in various kidney diseases by producing chemokines such as regulated upon activation, normal T cell expressed and secreted (RANTES) (16), and this is more pronounced in the presence of IFN-γ than IL-1 or TNF-α (17). Moreover, the level of proteinuria, which is independent of mean arterial BP, is reportedly one of the best predictors for disease progression toward end-stage renal failure (18,19). Microalbuminuria is known as an important early sign of diabetic nephropathy (20,21) and of progressive loss of renal function in the nondiabetic population (22). Recent studies have shown that proximal tubular cells are activated by reabsorption of abundant urinary proteins filtered through the glomerular capillaries, producing various chemokines that lead to kidney disease progression (23). Identification of the signal transduction pathway in activated proximal tubular cells is, however, still incomplete.

To study changes in *in vivo* gene expression in proximal tubular cells caused by proteinuria, we constructed an expression profile of proximal tubular cells isolated from an albumin-overloaded proteinuria mouse model by use of the body map procedure (24–29). These data showed that the expression patterns in proximal tubular cells were changed dramatically

Received March 28, 2003. Accepted October 31, 2003.
Correspondence to: Dr. Masaru Takenaka, Department of Internal Medicine and Therapeutics (Box A8), Osaka University Graduate School of Medicine, Osaka, 565-0871, Japan. Phone: +81787314416; Fax: +81787325161; E-mail: masaru@suma.kobe-wu.ac.jp

1046-6673/1502-0276
Journal of the American Society of Nephrology

DOI: 10.1097/01.ASN.0000109672.83594.02

by proteinuria. In view of the renal damage caused by proteinuria, it is of considerable interest that several immunity-related genes, including interferon regulatory factor–1, major histocompatibility complex (MHC) class I, MHC class II, and monocyte chemoattractant protein–1 (MCP-1), were found to be upregulated (26). These proteinuria-induced genes are likely to participate in kidney disease progression, and it is noteworthy that almost all of them are also induced by IFN-γ (30).

Although IFN-γ is essentially a cytokine with direct antiviral activity, its properties also include regulation of the immune response, antigen presentation of phagocytes through the MHC class I and II pathways, and orchestration of leukocyte-endothelium interactions through an intermediary in the JAK/STAT signaling pathway (30). Hence, we were interested in the relationship between the STAT family and proteinuria-initiated gene expression in proximal tubular cells.

In previous *in vitro* experiments, protein-overloaded proximal tubular cells were found to activate transcription of a number of genes encoding inflammatory molecules (31,32). However, the signaling pathways involved have not been analyzed in detail. Because it is likely that many inflammatory cytokines have various effects on the later stages of these pathways, we have focused mainly on the early stage to avoid such complications.

In this report, we present our results showing that albumin *per se* can generate ROS in proximal tubular cells, resulting in the activation of the STAT signaling pathway. We suggest that the membrane-bound NADPH oxidase system is important as an ROS generating system. Albumin-induced activation of Stat1 and Stat5 in murine proximal tubular cells (mProx24) cells was found to be mediated mostly by Jak2, without the need for protein synthesis.

Materials and Methods

Antibodies

The Stat1, Stat3, Stat5, phospho-Stat1 (Y701), phospho-Stat3 (Y705) and phospho-Stat5 (Y694) antibodies were purchased from Cell Signaling (Beverly, MA). The Jak1, Jak2, and phospho-Jak2 (Y1007/Y1008) antibodies were obtained from Upstate Biotechnology (Lake Placid, NY), and the phospho-Jak1 (Y1022/Y1023) antibody from Affinity BioReagents (Golden, CO). The Tyk2 and phospho-Tyk2 (Y1054/Y1055) antibodies were obtained from Santa Cruz Biotechnology (Santa Cruz, CA), and anti-murine IFN-γ antibody from Peprotech (Princeton, NJ).

Chemicals

Cycloheximide (CHX) and AG490 were purchased from Calbiochem (La Jolla, CA). Protein A agarose beads, nylon membranes (hybond-P) for Western blot test and, Hyperfilm ECL films were obtained from Amersham Pharmacia Biotech (Buckinghamshire, UK) and nylon membranes (Biodyne B) for electrophoretic mobility shift assays from Pall (East Hills, NY). The Pierce Supersignal substrate chemiluminescence detection kit and the BCA Protein Assay Reagent kit were purchased from Pierce Biotechnology (Rockford, IL). 5- (and 6-) Chloromethyl-2', 7'-dichlorodihydrofluorescein diacetate (CM-H_2DCFDA) was purchased from Molecular Probes (Eugene, OR), FCS and L-glutamine from InVitrogen (Carlsbad, CA), and Complete Mini from Boehringer Mannheim (Mannheim, Germany). Complete Mini tablets inhibit a broad spectrum of serine, cysteine, and metalloproteases as well as calpains. BSA (Fraction V, IgG free, low endotoxin), apo-transferrin (apoTf), *N*-acetyl-L-cysteine (NAC), diphenylene iodonium chloride (DPI), and all other chemicals were purchased from Sigma Chemical (St. Louis, MO).

Cells and Cell Culture

The murine proximal tubular cells (mProx24 cells derivative; patent WO9927363, JP, US, EU) (33,34) were cultured in DMEM/F-12 medium containing 10% FCS. The mProx24 cells were examined beforehand to determine whether they could produce a valid activation of STATs in response to IFN-γ and IL-6. We used FITC-labeled BSA to confirm their ability to generate albumin endocytosis (data not shown). In addition, we verified the upregulation of some genes induced by IFN-γ when albumin was added to the medium (data not shown).

Confluent mProx24 cells were rinsed three times with serum-free medium and starved in the serum-free medium for 24 h to eliminate the effect of FCS. mProx24 cells were then treated with albumin (30 mg/ml medium). Albumin mediums were filtered with a 0.22-μm filter unit (Millipore, Carrigtwohill, County Cork, Ireland) and polymyxin B was added suppress the influence of lipopolysaccharide. When drugs or antibodies were added, mProx24 cells were pretreated with the drugs or antibodies for 1 h before exposure to albumin. The concentration (0.05 ng/ml) of anti–IFN-γ antibody was determined according to the manufacturer's instructions. This concentration resulted in a valid inhibition of Stat1-activation by IFN-γ (data not shown).

Trypan Blue Uptake Test

To evaluate cell viability by trypan blue dye exclusion, mProx24 cells were treated with the antioxidants, NAC (20 mM), rotenone (10 μM), or DPI (10 μM) 1 h before and during the 30-min incubation with albumin (30 mg/ml). At the end of the stimulation, the cells were rinsed three times with ice-cold PBS, detached with trypsin, and resuspended in medium diluted 1:20 with trypan blue solution. Live cells and stained dead cells were then counted by a hemocytometer.

Immunoprecipitation, SDS-PAGE, and Western Blot Analysis

At the end of the treatment with albumin, the cells were rinsed three times with ice-cold PBS with 1 mM Na_3VO_4, solubilized in ice-cold lysis buffer (50 mM Tris-HCl, pH 7.4, 150 mM NaCl, 1% NP40, 0.25% sodium deoxycholate, 1 mM EDTA, 1 mM PMSF, 1 mM Na_3VO_4, 1 mM NaF, Complete Mini), and rotated for 1 h at 4°C. The total cell lysates were centrifuged at 14,000 × *g* for 10 min at 4°C. They were then incubated with the relevant antibody on ice for 2 h, and the antibody complexes were collected on protein A agarose beads during a 1-h incubation at 4°C. The beads were washed three times with the lysis buffer and boiled for 20 min in SDS-PAGE sample buffer. A total of 50 μg of each sample was separated by 7% SDS-PAGE and transferred to a nylon membrane (Hybond-P), where it was blocked by a 30-min incubation at room temperature in TPBS (20 mM Tris-HCl, pH 7.6, 137 mM NaCl, 0.05% Tween-20) plus 5% BSA and incubated overnight at 4°C with the relevant primary antibody. Subsequently, the membranes were washed three times for 5 min each with TPBS and incubated for 30 min with HRP-conjugated goat anti-rabbit IgG. After extensive washing, the bound antibody was visualized on Hyperfilm ECL film. Membranes were then incubated at 55°C for 30 min in stripping buffer (100 mM 2-ME, 2% SDS, 62.5

mM Tris-HCl, pH 6.8) to prepare them for a second round of immunoblotting.

Preparation of Nuclear Extracts and Electrophoretic Mobility Shift Assay (EMSA)

After the indicated treatment, the cells were rinsed three times with ice-cold PBS containing 1 mM Na_3VO_4, scraped from the dish and pelleted at 14,000 × *g* for 1 min at 4°C. Cells were then resuspended in the same buffer and pelleted as described above. The resultant pellets were resuspended in 400 μl of ice-cold buffer A (10 mM HEPES-KOH pH 7.8, 10 mM KCl, 0.1 mM EDTA pH 8.0, 0.1% NP-40, 1 mM DTT, 0.5 mM PMSF, 1 mM Na_3VO_4, Complete Mini). The lysate was vortexed vigorously for 20 s, and the nuclei were pelleted at 14,000 × *g* for 1 min at 4°C, followed by resuspension of the nuclear pellets in 100 μl of buffer C (50 mM HEPES-KOH pH 7.8, 420 mM KCl, 0.1 mM EDTA pH 8.0, 5 mM $MgCl_2$, 20% glycerol, 1 mM DTT, 0.5 mM PMSF, 1 mM Na_3VO_4, Complete Mini) and rotation for 1 h at 4°C. The extracted proteins were separated from the residual nuclei at 14,000 × *g* for 15 min at 4°C, and the supernatant fractions were used as nuclear extracts. EMSA was performed with the Panomics' EMSA Kit (Panomics, Redwood City, CA) according to the manufacturer's instructions.

Assessment of Intracellular ROS

Intracellular ROS generation was assessed in mProx24 cells by means of an oxidant-sensitive dye, CM-H_2DCFDA. Suspensions of the cells (10^6 cells) were incubated with 5 μM CM-H_2DCFDA for 15 min at 37°C in the serum-free medium. After centrifugation and washing to remove unincorporated probe, cells were treated with several concentrations of albumin medium for 15 min at 37°C and placed on ice. Mean fluorescence intensity of DCF in the cells was measured by a flow cytometer (FACSCalibur; Becton Dickinson Biosciences, Franklin Lakes, NJ).

Measurement of SOD, Glutathione Peroxidase, and Catalase Activities, and the Total Reduced Form of Glutathione

The SOD activity was measured with a Superoxide Dismutase Assay Kit (Trevigen, Gaithersburg, MD). The cellular glutathione peroxidase (GPx) activity was determined with a Bioxytech GPx-340 (OxisResearch, Portland, OR). The catalase activity was measured with an Amplex Red Catalase Assay Kit (Molecular Probes, Eugene, OR). The total reduced form of glutathione (GSH) was determined with a Bioxytech GSH-400 (OxisResearch). Each of the kits was used according to the manufacturer's instructions.

Results

Activation of STATs in mProx24 Cells by Albumin

We first investigated whether members of the STAT family were activated by albumin. mProx24 cells were treated with albumin (30 mg/ml medium) for various lengths of time. Western blot analyses showed that Stat1 and Stat5 were rapidly activated within 15 min of exposure to albumin, with Stat5 in particular showing early and obvious activation. Stat3, however, demonstrated no detectable activation after 15 min (Figure 1A). To confirm Stat1 and Stat5 activation, nuclear extracts were prepared from the albumin-treated cells and analyzed by EMSA. This approach also showed rapid activation of Stat1 and Stat5 within 15 min of exposure to albumin. These results were finally confirmed by competition and supershift analyses (Figure 1B). To verify the later activation of Stat3 after albumin overloading, mProx24 cells were treated with albumin for longer lengths of time. Western blot analyses showed that Stat3 activation occurred only after a 4-h exposure to albumin (Figure 1C).

Activation of Albumin-Induced STATs through Jak2

The rapid phosphorylation of Stat1 and Stat5 indicated that albumin is, like cytokines, a direct stimulant of the JAK family. We examined the time courses of the phosphorylation of Jak1, Jak2, and Tyk2 in albumin-overloaded mouse mProx24 cells. Western blot analyses showed that rapid activation of Jak2 took place within 15 min of exposure to albumin, compared with no obvious activation of Jak1 or Tyk2 (Figure 2A). To confirm that the activation of Stat1 and Stat5 was under the control of Jak2, we tested the effect of AG490 (20 μM), a specific inhibitor of Jak2. The results in Figure 2B indicate that AG490 inhibited the activation of Jak2 and prevented the activation of Stat1 and Stat5, compared with the control. Given the strong evidence that JAK kinases are *in vivo* STAT kinases (35), our results suggest that the albumin-induced activation of Stat1 and Stat5 in mProx24 cells was mediated mostly by Jak2.

Moreover, to investigate whether protein synthesis was involved in the activation of Stat1 and Stat5, we tested the effect of CHX (2 μg/ml), a protein synthesis inhibitor. The results in Figure 3A indicate that CHX did not affect the albumin-induced Tyr-phosphorylation of STATs within 15 min, thus demonstrating that the albumin-induced activation of Stat1 and Stat5 occurred without protein synthesis.

Although the JAK/STAT signaling pathway appeared to be activated by albumin *per se*, some cytokines and/or growth factors may have been involved in this phenomenon. Hence, the effect of an inhibitory antibody on the JAK/STAT signaling pathway was examined. It is well known that Jak2 fulfills an essential function in response to IFN-γ (36). We therefore used an anti–IFN-γ antibody (0.05 ng/ml) as a representative cytokine-neutralization antibody to check whether albumin could induce IFN-γ secretion from mProx24 cells. mProx24 cells were pretreated with anti-IFN-γ antibody for 1 h before exposure to albumin. The results indicated that anti–IFN-γ antibody did not prevent the albumin-induced Tyr-phosphorylation of Stat1, suggesting that the albumin-induced activation of Stat1 was not a direct effect of IFN-γ (Figure 3B).

Activation of STATs in mProx24 Cells Was Not Specific to Albumin

To investigate whether the activation of the STATs was specific to albumin, mProx24 cells were treated with apoTf (30 mg/ml medium) for 15 min. ApoTf is one of the major components of plasma proteins and consists of transferrin that is not saturated with iron. Western blot analyses showed that there was also rapid activation of Stat1 and Stat5 within 15 min of exposure to apoTf (Figure 4), indicating that the activation of the STATs was not albumin specific.

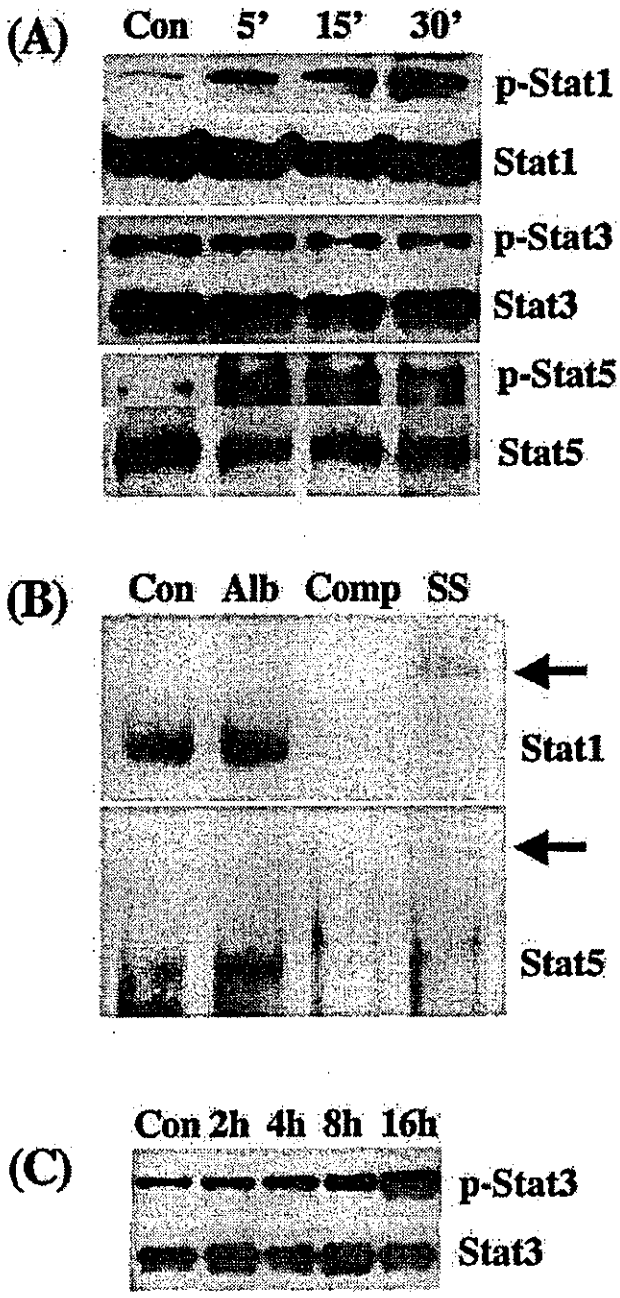

Figure 1. Western blot analysis and electrophoretic mobility shift assays (EMSA) of activated Stat1 and Stat5 in mouse renal proximal tubular cells (mProx24 cells) treated with albumin. mProx24 cells were treated with albumin for various time periods. (A) Western blot analyses detected phosphorylated Stat1 and Stat5 15 min after addition of albumin, indicating that albumin could induce signal transducer and activator of transcription (STAT) signaling pathways. Stat3 showed no significant changes. Western blot analyses of Stat1, Stat3, and Stat5 are shown as controls. (B) EMSA confirmed rapid activation of Stat1 and Stat5 within 15 min of exposure to albumin. These results were confirmed by competition (Comp) and supershift (SS) analyses by using control samples. Band shifts are indicated by arrows. (C) Western blot detection of phosphorylated Stat3 4 h after addition of albumin. Western blot analysis of Stat3 are shown as controls. Three independent experiments were performed, and results are shown for one representative experiment.

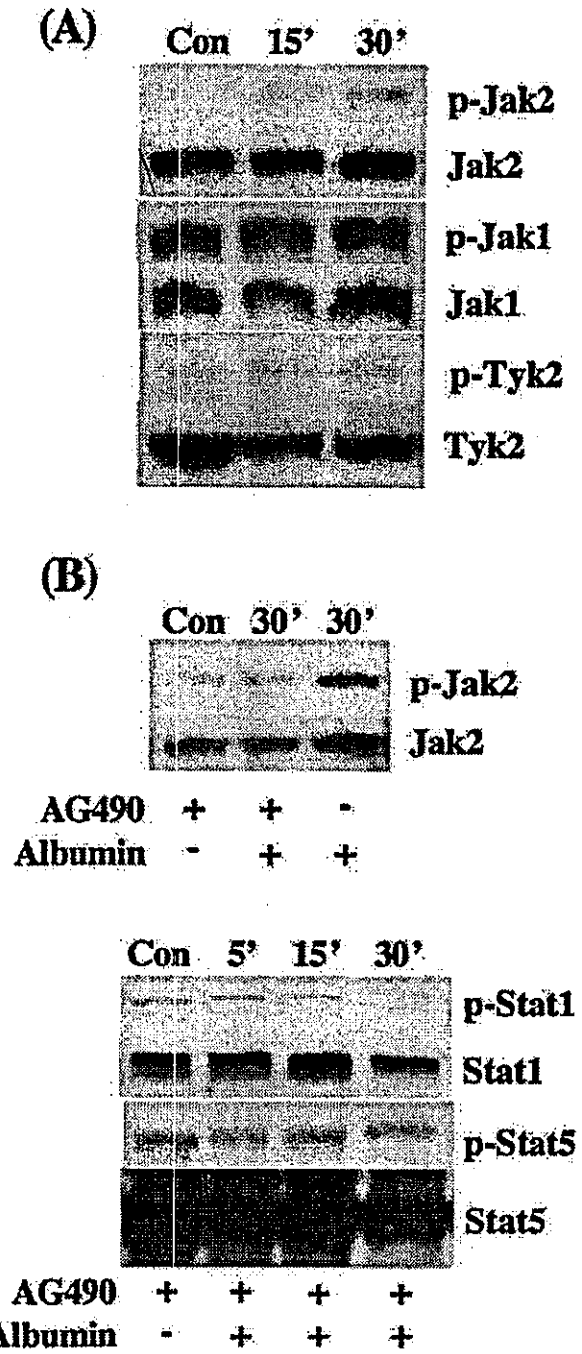

Figure 2. Activation of Jak2 in mouse renal proximal tubular (mProx24) cells treated with albumin mediates the activation of Stat1 and Stat5. (A) Phosphorylated Jak2 was detected 15 min after addition of albumin, demonstrating that albumin induced JAK signaling pathways. Jak1 and Tyk2 showed no significant changes. Western blot results for Jak2, Jak1, and Tyk2 are shown as controls. (B) mProx24 cells were transferred to a medium containing albumin (30 mg/ml medium) in the presence of AG490 (20 μM). AG490 inhibited the activation of Jak2 (only control and 30-min data shown) and prevented the activation of Stat1 and Stat5 compared with the control, indicating that albumin-induced activation of Stat1 and Stat5 was mediated mostly by Jak2. Western blot analyses for Stat1 and Stat5 are shown as controls. Three independent experiments were performed, and results are shown for one representative experiment.

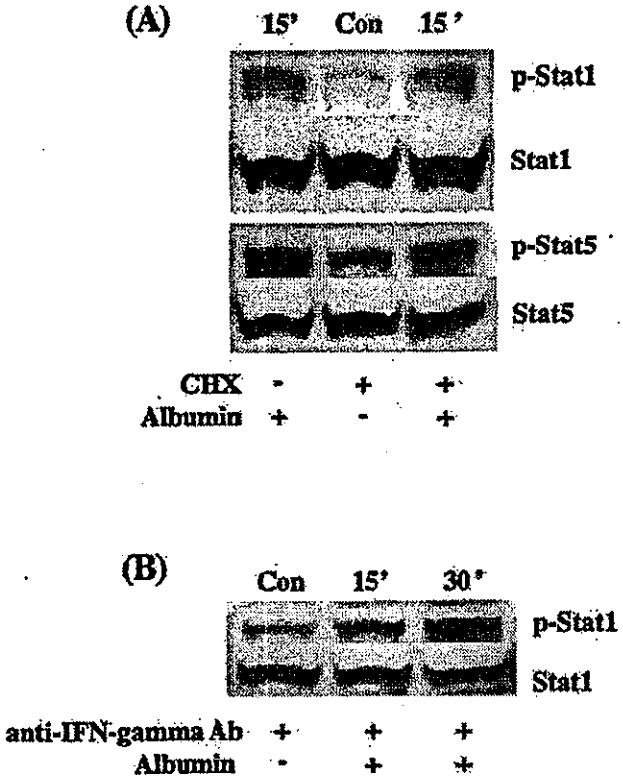

Figure 3. Effects of cycloheximide or anti–IFN-γ antibody on albumin-induced Stat1 and Stat5 activation. Mouse renal proximal tubular (mProx24) cells were transferred to a medium containing albumin (30 mg/ml medium) in the presence of cycloheximide (2 μg/ml) or anti–IFN-γ antibody (0.05 ng/ml). (A) Cycloheximide could not inhibit albumin-induced activation of Stat1 and Stat5. (B) Anti–IFN-γ antibody could not inhibit albumin-induced activation of Stat1. Three independent experiments were performed, and results are shown for one representative experiment.

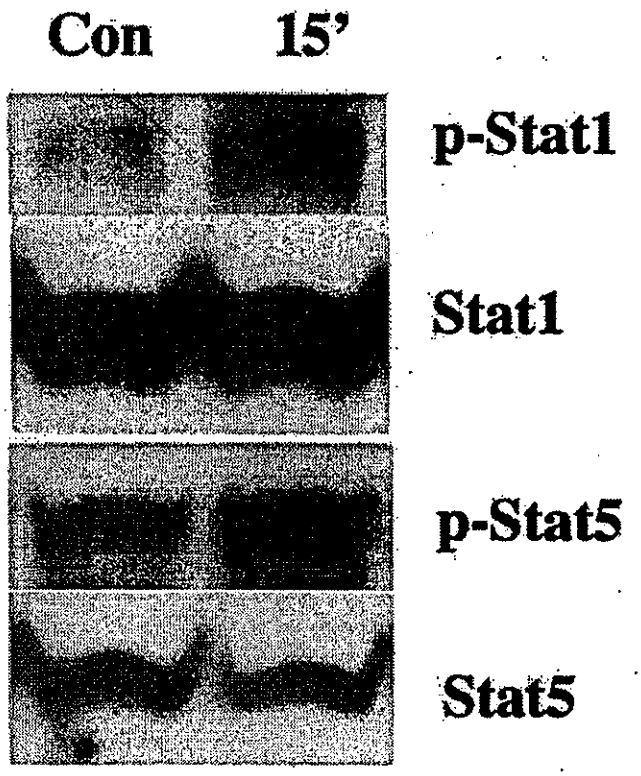

Figure 4. Western blot analyses of activated Stat1 and Stat5 in mouse renal proximal tubular (mProx24) cells treated with addition of apoTf. Phosphorylated Stat1 and Stat5 were detected 15 min after addition of apoTf, indicating that apoTf induced signal transducer and activator of transcription (STAT) signaling pathways. Western blot analyses for Stat1 and Stat5 are shown as controls. Three independent experiments were performed, and results are shown for one representative experiment.

Assessment of ROS Generation by Albumin and apoTf

Recently, it was reported that albumin upregulated ROS generation in proximal tubular cells (37,38). Therefore, to directly assess whether albumin could induce oxidative stress in mProx24 cells, we used the CM-H_2DCFDA method and fluorescence-activated cell sorter (FACS) analysis. After CM-H_2DCFDA incubation, mProx24 cells were treated with albumin for 15 min. Accumulation of DCF in mProx24 cells was measured with a flow cytometer by monitoring the fluorescence at 526 nm (39). ROS generation was found to be upregulated compared with the control within 15 min after either albumin or apoTf had been added to the medium (Figure 5). Dose-dependent upregulation of intracellular ROS generation was observed, as previously reported (37). The result was not changed by addition of DMSO, which was used as the solvent for AG490, rotenone, and DPI (data not shown).

To inhibit ROS generation by albumin, we checked the effect of NAC (20 mM), a precursor of GSH and a ROS scavenger, rotenone (10 μM), an inhibitor of complex I of the mitochondrial respiratory chain, and DPI (10 μM), an inhibitor of membrane NADPH oxidase. All three were able to block ROS generation by albumin (Figure 5). These results supported our finding that albumin could induce oxidative stress in mProx24 cells. ROS generation was observed even in the control mProx24 cells after starvation, compared with the findings with antioxidants.

Activation of Albumin-Induced STATs through ROS

FACS analyses showed that albumin-induced ROS generation could be blocked by the three antioxidants. To determine whether the activation of Stat1 and Stat5 occurred by way of oxidative stress, we first tested the effect of NAC (20 mM). The results presented in Figure 6 indicate that NAC prevented albumin-induced Tyr-phosphorylation of Stat1 and Stat5 within 15 min (Figure 6, A and B). Moreover, even the activation of Stat1 and Stat5 in the control cells was suppressed by pretreatment with NAC (Figure 6A). This suggests that the activation of Stat1 and Stat5 could take place through the upregulation of ROS generation.

The mitochondrial respiratory chain is one of the major intracellular sources of ROS and indispensable to cell function.

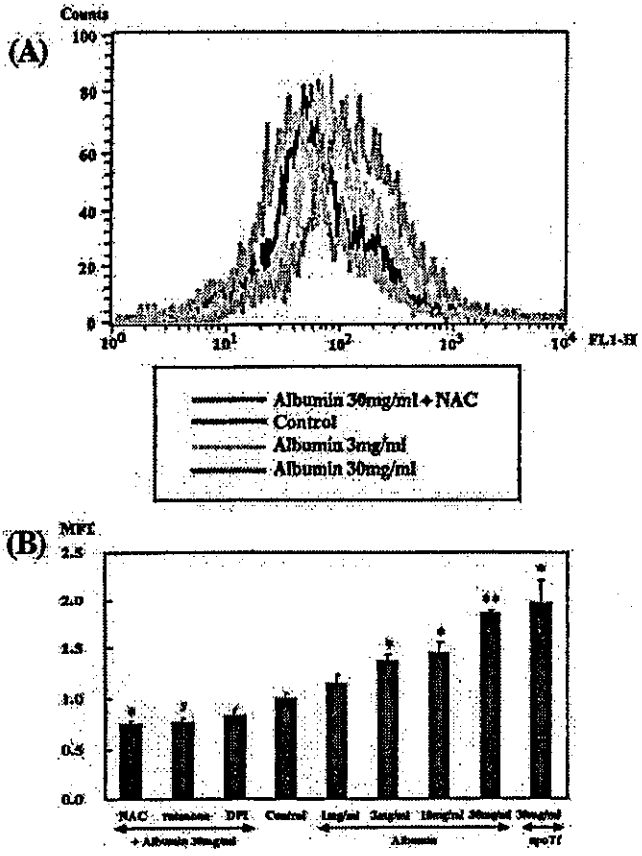

Figure 5. Assessment of reactive oxygen species (ROS) by fluorescence-activated cell sorter analysis. After CM-H_2DCFDA incubation, mouse renal proximal tubular (mProx24) cells were treated with albumin for 15 min. Accumulation of DCF was measured with a flow cytometer by monitoring fluorescence at 526 nm. The increase was assumed to be proportional to the concentration of superoxide anions and hydrogen peroxide in the mProx24 cells. (A) Results are shown for one representative experiment. ROS generation was observed even in the control mProx24 cells (black line). The ROS generation was upregulated within 15 min after albumin (yellow line; 3 mg/ml, blue line; 30 mg/ml) overloading, but NAC (green line), a precursor of glutathione (GSH) and a ROS scavenger, blocked ROS generation. (B) Intracellular ROS formation was expressed as a ratio of the mean fluorescence intensity of control cells incubated in an albumin-free medium. Results are the means ± SD of triplicate experiments. $\$P <$ 0.01 *versus* control cells. $*P < 0.005$ *versus* control cells. $**P <$ 0.001 *versus* control cells.

We investigated the involvement of mitochondria in the albumin-induced ROS with an inhibitor of the mitochondrial respiratory chain, rotenone (10 μM). The results showed that rotenone prevented the albumin-induced Tyr-phosphorylation of Stat1 and Stat5 within 15 min, compared with the positive control (Figure 7, A and B). Pretreatment with rotenone also suppressed the activation of Stat1 and Stat5 in the control cells (Figure 7B). This indicated that inhibition of the mitochondrial respiratory chain could suppress ROS generation by albumin or by starvation.

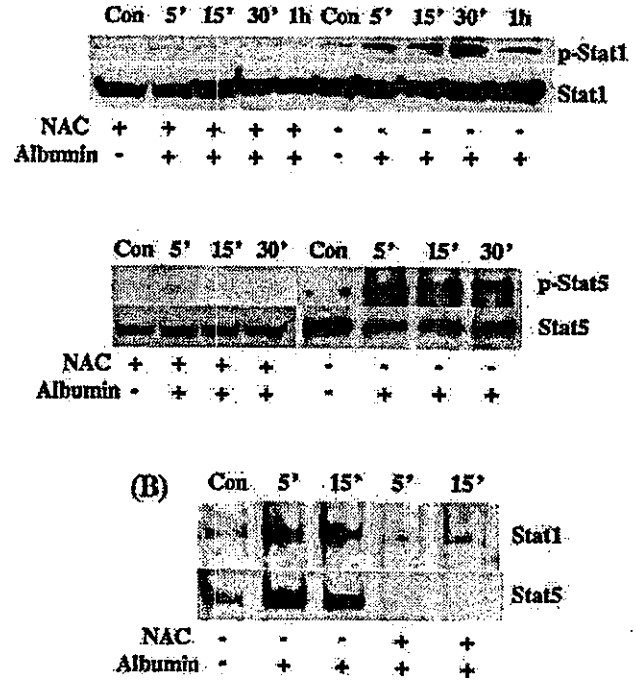

Figure 6. Effects of *N*-acetyl-L-cysteine (NAC) on albumin-induced Stat1 and Stat5 activation. Mouse renal proximal tubular (mProx24) cells were transferred to a medium containing albumin (30 mg/ml medium) in the presence of NAC (20 mM). (A) Western blot analyses showed that activation of Stat1 and Stat5 was inhibited by NAC, indicating that the activation of Stat1 and Stat5 is mediated by reactive oxygen species (ROS). Western blot analyses for Stat1 and Stat5 are shown as controls. (B) Electrophoretic mobility shift assay (EMSA) also confirmed the inhibition of Stat1 and Stat5 by NAC. Three independent experiments were performed, and results are shown for one representative experiment.

Intracellular generation of ROS in response to ligands is often mediated by the activity of membrane-bound NADPH oxidase (40,41). DPI (10 μM) also prevented the albumin-induced Tyr-phosphorylation of Stat1 and Stat5 (Figure 7, A and C), but did not seem to suppress the activation of Stat1 and Stat5 in the control cells (Figure 7C). This suggests that ROS generated by albumin are mainly derived from the membrane-bound NADPH oxidase system.

Because pretreatment with NAC and rotenone even suppressed the activation of Stat1 and Stat5 in the control cells, we evaluated the cell viability in the presence of NAC, rotenone and DPI by trypan blue dye exclusion. The antioxidants did not have much effect on cell viability, at least during the 30-min incubation with albumin (30 mg/ml) (Table 1).

Measurement of SOD, GPx, and Catalase Activities

The membrane-bound NADPH oxidase system produces superoxide anions in cells, and intracellular SOD is the main enzyme that metabolizes these anions. Because interference with the SOD activity could induce accumulation of superoxide anions, we measured the SOD activity after mProx24 cells had been treated with albumin for 10 min. No marked change

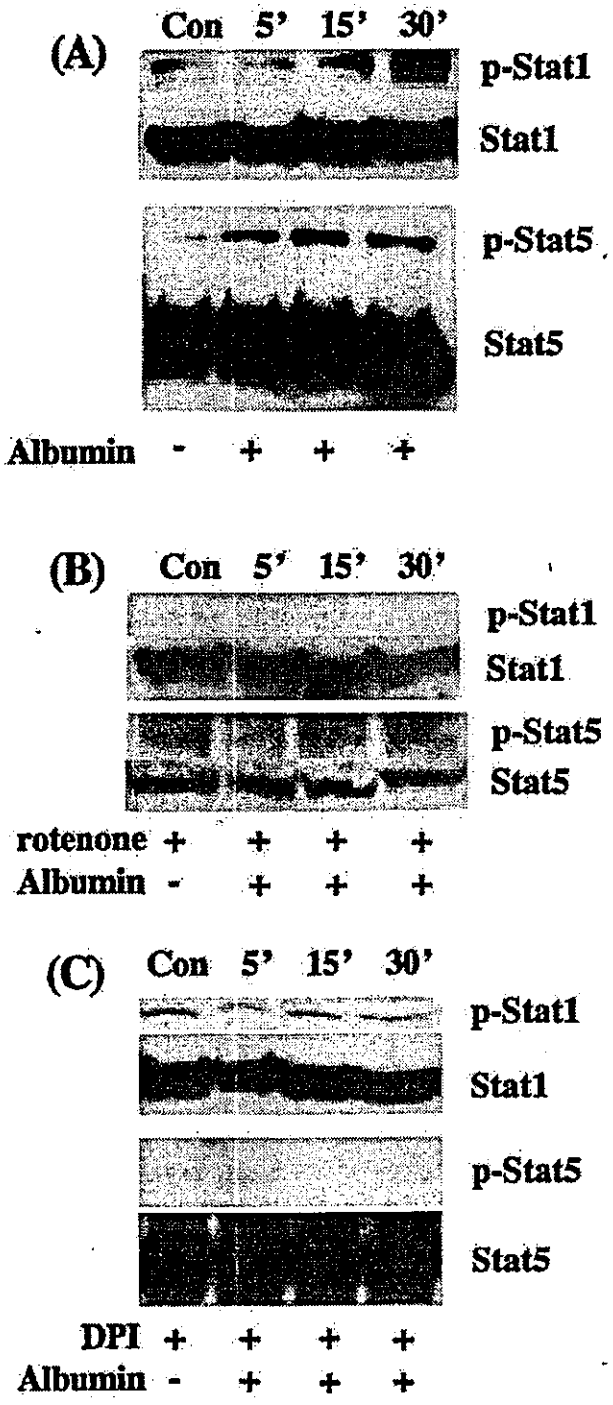

Figure 7. Effects of rotenone or diphenylene iodonium chloride (DPI) on albumin-induced Stat1 and Stat5 activation. Mouse renal proximal tubular (mProx24) cells were transferred to a medium containing albumin (30 mg/ml medium) in the presence of rotenone (10 μM) or DPI (10 μM). Western blot analyses showed that activation of Stat1 and Stat5 was inhibited by either rotenone (B) or DPI (C), compared with the positive control (A), indicating that the activation of Stat1 and Stat5 was mediated by reactive oxygen species (ROS). Western blot analyses for Stat1 and Stat5 are shown as controls. Three independent experiments were performed, and results are shown for one representative experiment.

Table 1. Viable cell count by trypan blue dye exclusion

	% of Control
Control	100.00
Albumin	103.84 ± 3.18
Albumin + NAC	102.29 ± 2.96
Albumin + rotenone	102.67 ± 4.42
Albumin + DPI	99.66 ± 2.12

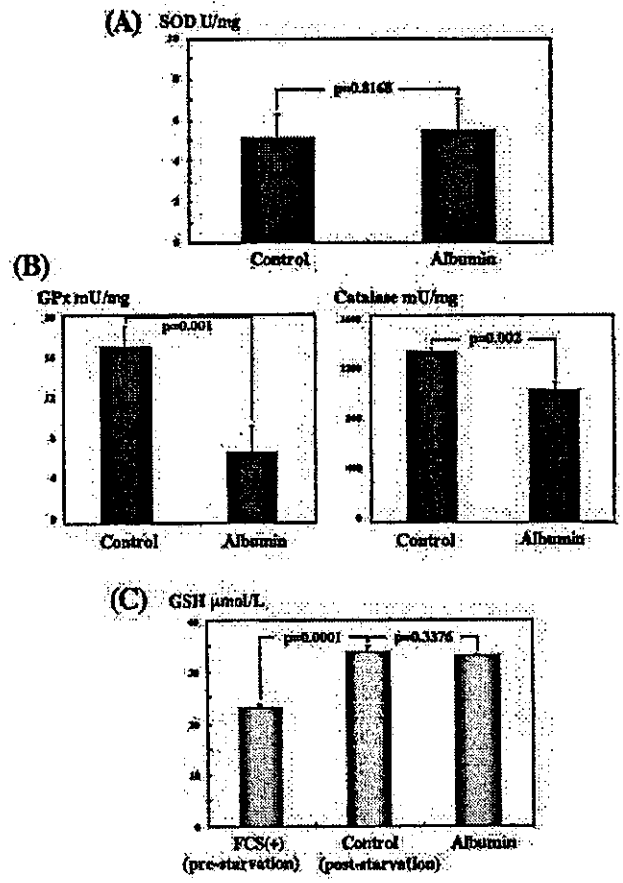

Figure 8. Measurement of SOD, glutathione peroxidase (GPx), and catalase activity, and the total reduced form of Glutathione. (A) SOD activity was measured after 10-min albumin treatment of mouse renal proximal tubular (mProx24) cells, but showed no significant change. (B) GPx and catalase activities were measured after 10-min albumin treatment of mProx24 cells. Both GPx and catalase activities were reduced after albumin overloading. (C) Quantity of total glutathione (GSH) was determined after 10-min albumin treatment of mProx24 cells. The quantity increased after starvation but showed no significant change after treatment with albumin compared with control. The histograms represent the means of three independent experiments (means ± SD).

was observed (Figure 8A). These results indicate that altered SOD activity was not responsible for the accumulation of intracellular ROS after exposure of mProx24 cells to albumin.

SOD produces hydrogen peroxide in cells, and intracellular GPx and catalase are the main enzymes that convert hydrogen